Accelerating the convergence of AFETI partitioned analysis of heterogeneous structural dynamical systems

José A. González[a,*], K. C. Park[b]

[a] *Escuela Técnica Superior de Ingeniería, Universidad de Sevilla, Camino de los Descubrimientos s/n, Sevilla 41092, Spain*
[b] *Ann and H. J. Smead Aerospace Engineering Sciences, University of Colorado, Boulder, CO 80309-429, USA*

Abstract

Variationally based algorithms for the partitioned solution of structural mechanics problems are presented. Two key features of the present algorithms are the judicious application of the *d'Alembert-Lagrange principal equations* and the use of dominant substructural deformation modes. The paper includes three developments:

1. Variational derivation of AFETI parallel solution methods.
2. One-level and two-level AFETI implicit transient analysis algorithms with coarse problem included in the projector and based on free floating rigid body modes.
3. A new AFETI implicit transient solution algorithm derived by constraining the interface equilibrium equations with the floating and dominant deformational modes.

In addition to variational derivations of solution algorithms, the present paper is strived to offer new physical and/or numerical insight as each of variational derivational steps is succinctly explained. Performance evaluations of the algorithms described herein are presented.

Keywords: FETI method, localized Lagrange multipliers, partitioned analysis, heterogeneous systems

1. Introduction

It is by now a well established practice to employ variational principles (e.g., [1, 2, 3, 4, 5, 6]) in the finite element discretization of continuum structural models. Once the discrete equations are generated, the prevailing practice in the solution of the discrete model equations is to leave the variational framework behind and adopt matrix algebraic solvers. This transition phase from variational approaches for the equation generation to algebraic solution procedures is justified when the resulting matrix equation can be efficiently treated in the standard form of a linear system, for which there exist a host of

*Corresponding author
Email addresses: japerez@us.es (José A. González), kcpark@colorado.edu (K. C. Park)

solution methods. The growing interest in the modeling and parallel solution algorithms development for large-scale structural systems or multi-physics problems has prompted a number of solution algorithms developers to employ matrix algebraic utilities [7, 8, 9].

The present paper is an attempt to utilize variational framework as much as possible in the development of solution algorithms for parallel computations of structural mechanics and multi-physics or coupled-field problems. In that sense the paper may be viewed a sequel to our earlier work [10, 11, 12, 13, 14, 15] which may be regarded collectively as a precursor to truly variational derivations of solution algorithms. Others may view our attempt to utilize variational framework for solution methods development a daunting effort. We believe we have two historical precedents in our favor. One is the gradual transition from the matrix structural analysis to variational treatment in the construction of finite elements; and, the other is from the use of finite difference methods in the development of transient time integration algorithms to the direct time discretization of Hamilton's principle.

The underlying theme of our variational derivation of solution algorithms is the partitioned modeling and analysis where a partition is defined as a spatial subdivision based on physics; for example, a seismic excited dam model might be divided into a fluid, a structure and a soil partition [16, 17]. A partitioned subdomain interacts with its adjacent subdomains through the interface forces and moments or Lagrange multipliers. The treatment of Lagrange multiplier-connected components of a mechanical system has been addressed by many authors, particularly in multibody dynamics [18, 19, 20], parallel computation [21, 22, 23, 24, 25, 26, 27, 28, 29, 30, 31, 32], multistep integration [33, 34], contact problems [35, 36] and multiphysics simulation [37, 38, 16, 39].

It is well known that the self-equilibrium equations for each partition or the *d'Alembert-Lagrange principal equations*, play a pivotal role in the variational derivation of solution methods [40]. We should mention that they have been utilized in the formulation of classical force method for relating the reaction forces to the applied forces [1, 41], in the development of finite elements [42, 43] for satisfying zero-strain modes, in the solution of singular systems for quasi-static problems [44], and for the parallel solution of static linear structures [21]. We take the view that a full potential use of the d'Alembert-Lagrange principal equations for the development of partitioned solution algorithm is still wanting, especially for dynamic problems.

The benefits of using the rigid body modes to accelerate the convergence of implicit transient FETI methods, were first reported by Farhat et. al. [45] for second order elasticity problems. It was demonstrated that, by introducing the floating or rigid-body motions into the projector, the condition number κ of the interface problem and consequently the number of iterations, deteriorates at most logarithmically

with the number of elements per substructure:

$$\kappa \approx \mathcal{O}\left(1 + \log^m\left(\tfrac{H}{h}\right)\right), \quad m \leq 3 \tag{1}$$

where H indicates the size of the subdomains and h denotes the size of the elements. Note that this condition number estimate is independent of the number of subdomains, a necessary condition to achieve numerical scalability. The same optimality bound was later achieved for fourth order plates and shell elements [25] by enforcing continuity of the transverse displacement field at the substructure corners throughout the preconditioned conjugate projected gradient iterations. In the context of AFETI methods [10, 11, 13, 14, 46], we will see that for optimal convergence of fourth order problems, corner constraints can be substituted by complete interface deformational modes plus regularization.

In an effort to create a common solver applicable for both static and dynamic analyses, Farhat and his coworkers eventually succeeded in developing the FETI-DP algorithm [31, 47] whose solver is not only applicable to both static and dynamic problems but also significantly improves the solution efficiency. In the FETI-DP algorithm, the interface nodes are divided into a selected set of corner nodes and a remaining set of boundary nodes. The corner nodes are used to formulate a primal interface problem, maintaining the corner displacement DOFs as unknowns, while the boundary nodes are utilized to formulate a coupled dual interface problem with classical Lagrange multipliers. Hence, the corner nodes form a coarse finite element representation of the global problem that ensures scalability by propagating local substructure equilibrium globally, eliminating the need for introducing rigid body modes in the formulation. Nowadays, two-level FETI-DP method is the *de facto* parallel algorithm for solid and structural mechanics, that has demonstrated optimal numerical and parallel scalability properties up to billions of DOFs [48].

The paper is organized as follows. Section 2 begins with the variational formulation of partitioned equations of motion for structures employing the method of localized Lagrange multipliers, leading to three-variable equations of motion. The substructural displacement is decomposed into deformational attributes and rigid-body motions, leading to four-variable partitioned equation set. Utilizing the implicit time discretization of the three or four-variable partitioned equations of motion, previously developed AFETI algorithms are reviewed in Sections 3 and 4. The importance of rigid-body modes (RBMs), referred to *d'Alembert-Lagrange principal equations*, is elucidated in Section 5. Specifically, it is shown that the rigid-body components of the residual of the interface force equilibrium equations dictate the substructure-by-substructure global equilibrium. This suggests that the rigid-body modes constitute the principal constraint on the interface force equilibrium.

A culminating stage of the present paper is the development of a new AFETI algorithm, labelled as AFETI-C, presented in Section 6. We believe that AFETI-C is simple to understand and easy to implement. In essence, AFETI-C utilizes a combination of rigid-body modes and dominant substructural deformation modes in enforcing the interface force equilibrium equation as constraint conditions. In addition, a regularization of heterogeneities of partitioned systems [13, 14, 49] is appended to AFETI-C to treat fourth order structural problems. Section 7 presents the performance of AFETI-C compared with some of the existing algorithms, illustrating the good performance of AFETI-C with regularization. Finally, we note that the solver presented in this paper is applicable to a large family of time-dependent problems, providing convergence acceleration with minimum implementation complications.

2. Variational derivation of AFETI methods

In this section, the classical AFETI methods are derived from the same variational form, proposing different decompositions for the localized Lagrange multipliers using selected projectors that will give place to the diverse AFETI variants.

We have observed that the fundamental solution of a floating structural dynamical system is given by the corresponding rigid-body modes. For structural dynamical problems to be treated by partitioned subsystems, the basic solution components of the interface Lagrange multipliers are also governed by the rigid-body modes. To this end, we first derive the equations of motion for a partitioned structural system. The explicit inclusion of the floating modes then follows.

2.1. Partitioned equations for a linear structural dynamical system

To derive the partitioned equations of motion of a linear structural dynamical system, we use the variational formulation proposed by Park and Felippa [12, 15] where the problem is treated like if all bodies were entirely free. Then, the total virtual work of the complete system is obtained by summing up the contributions of each substructure, plus the contribution of the interface constraints via the method of localized Lagrange multipliers:

$$\delta \mathscr{W}_t = \delta \mathscr{W}_d + \delta \mathscr{W}_c \tag{2}$$

terms corresponding to the virtual work of the free-floating substructures and localized interface constraints, respectively.

The displacement-based discrete energy functional $\mathscr{W}_d(\mathbf{u})$, for a group of N free-floating linear

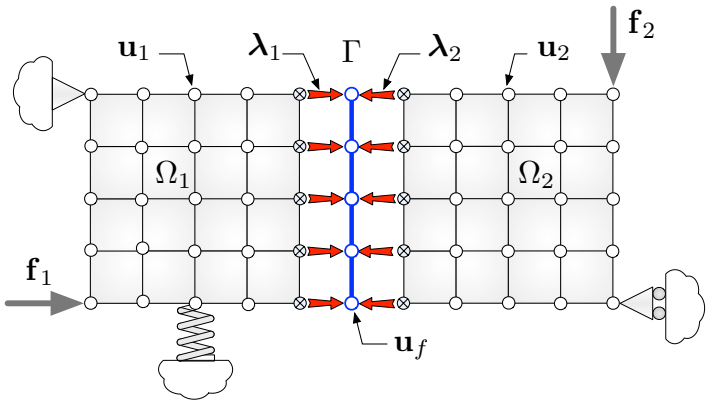

Figure 1: Connection of two substructures using localized Lagrange multipliers. Localized Lagrange multipliers introduce an explicit definition of the interface with its own DOFs denominated frame. Multipliers localization avoid the non-unique definition problem presented by classical Lagrange multipliers at corner and cross-points.

undamped substructures under dynamic loading, can be expressed in matrix form as:

$$\delta \mathscr{W}_d \left(\mathbf{u}\right) = \sum_{i=1}^{N} \delta \mathscr{W}_{d_i} \left(\mathbf{u}_i\right) = \sum_{i=1}^{N} \delta \mathbf{u}_i^{\mathsf{T}} \left\{\mathbf{M}_i \ddot{\mathbf{u}}_i + \mathbf{K}_i \mathbf{u}_i - \mathbf{f}_i\right\} = \delta \mathbf{u}^{\mathsf{T}} \left\{\mathbf{M}\ddot{\mathbf{u}} + \mathbf{K}\mathbf{u} - \mathbf{f}\right\} \tag{3}$$

with the following definitions,

$$\mathbf{M} = \begin{bmatrix} \mathbf{M}_1 & \cdots & \mathbf{0} \\ \vdots & \ddots & \vdots \\ \mathbf{0} & \cdots & \mathbf{M}_N \end{bmatrix}, \quad \mathbf{K} = \begin{bmatrix} \mathbf{K}_1 & \cdots & \mathbf{0} \\ \vdots & \ddots & \vdots \\ \mathbf{0} & \cdots & \mathbf{K}_N \end{bmatrix}, \quad \mathbf{u} = \begin{Bmatrix} \mathbf{u}_1 \\ \vdots \\ \mathbf{u}_N \end{Bmatrix}, \quad \mathbf{f} = \begin{Bmatrix} \mathbf{f}_1 \\ \vdots \\ \mathbf{f}_N \end{Bmatrix} \tag{4}$$

where $\mathbf{u}$ is the partitioned subsystem-by-subsystem displacement vector, $\mathbf{f}$ the assembled vector of external forces, $\mathbf{K}$ and $\mathbf{M}$ are the block diagonal substructure-by-substructure stiffness and mass matrices, respectively, the subindex $i = 1, \ldots, N$ refers to partition number and the superscript dot denotes time differentiation.

The key to obtain a partitioned formulation of the problem is to treat the connection interfaces by the method of localized Lagrange multipliers that produces independent multipliers for each substructure. Specifically, see case represented in Figure 1 with $N = 2$ partitions, instead of carrying out a direct coupling of the two bodies, we will introduce an explicit representation of the interface boundary Γ, denominated *frame* in the AFETI literature, with its own displacement DOFs $\mathbf{u}_f$, and consider the coupling in terms of interaction of the substructures with the frame.

We can write the substructure-frame boundary displacement compatibility equations as:

$$\mathbf{B}_i^{\mathsf{T}}\mathbf{u}_i = \mathbf{L}_{fi}\mathbf{u}_f \quad (i = 1 \cdots N) \quad \Rightarrow \quad \begin{Bmatrix} \mathbf{B}_1^{\mathsf{T}}\mathbf{u}_1 \\ \vdots \\ \mathbf{B}_N^{\mathsf{T}}\mathbf{u}_N \end{Bmatrix} = \begin{Bmatrix} \mathbf{L}_{f_1} \\ \vdots \\ \mathbf{L}_{f_N} \end{Bmatrix} \mathbf{u}_f \tag{5}$$

where $\mathbf{B}_i$ is the Boolean assembly matrix corresponding to i^{th} substructure and $\mathbf{L}_{f_i}$ is the Boolean matrix relating the frame displacements $\mathbf{u}_f$ to the substructural displacements $\mathbf{u}_i$. These boundary constraints can be written in matrix form:

$$\mathbf{B}^{\mathsf{T}}\mathbf{u} - \mathbf{L}_f\mathbf{u}_f = \mathbf{0} \tag{6}$$

by making use of the block-matrices:

$$\mathbf{B} = \begin{bmatrix} \mathbf{B}_1 & \cdots & \mathbf{0} \\ \vdots & \ddots & \vdots \\ \mathbf{0} & \cdots & \mathbf{B}_N \end{bmatrix}, \quad \mathbf{L}_f = \begin{bmatrix} \mathbf{L}_{f_1} \\ \vdots \\ \mathbf{L}_{f_N} \end{bmatrix} \tag{7}$$

where $\mathbf{B}$ is the global boundary assembly operator and $\mathbf{L}_f$ is the frame-substructure interpolation matrix.

The partition interface constraint functional is simply obtained multiplying the boundary compatibility condition (6) by a field of Lagrange multipliers:

$$\mathscr{W}_{\mathrm{c}}\left(\mathbf{u}, \mathbf{u}_f, \boldsymbol{\lambda}\right) = \boldsymbol{\lambda}^{\mathsf{T}}\left\{\mathbf{B}^{\mathsf{T}}\mathbf{u} - \mathbf{L}_f\mathbf{u}_f\right\} \tag{8}$$

where $\boldsymbol{\lambda}^{\mathsf{T}} = \left[\boldsymbol{\lambda}_1^{\mathsf{T}} \cdots \boldsymbol{\lambda}_N^{\mathsf{T}}\right]$ represents the independent localized Lagrange multipliers of the substructures.

Finally, the total virtual work of the discrete partitioned system $\delta\mathscr{W}_t$ is derived combining (3) and (8) in the form:

$$\delta\mathscr{W}_t\left(\mathbf{u}, \mathbf{u}_f, \boldsymbol{\lambda}\right) = \delta\mathbf{u}^{\mathsf{T}}\left\{\mathbf{M}\ddot{\mathbf{u}} + \mathbf{K}\mathbf{u} - \mathbf{f}\right\} + \delta\left\{\boldsymbol{\lambda}^{\mathsf{T}}\left(\mathbf{B}^{\mathsf{T}}\mathbf{u} - \mathbf{L}_f\mathbf{u}_f\right)\right\} \tag{9}$$

and from the stationary-point condition of this virtual work, the partitioned equations of motion are obtained:

$$\begin{bmatrix} \mathbf{K} + \mathbf{M}\frac{d^2}{dt^2} & \mathbf{B} & \mathbf{0} \\ \mathbf{B}^{\mathsf{T}} & \mathbf{0} & -\mathbf{L}_f \\ \mathbf{0} & -\mathbf{L}_f^{\mathsf{T}} & \mathbf{0} \end{bmatrix} \begin{Bmatrix} \mathbf{u} \\ \boldsymbol{\lambda} \\ \mathbf{u}_f \end{Bmatrix} = \begin{Bmatrix} \mathbf{f} \\ \mathbf{0} \\ \mathbf{0} \end{Bmatrix} \tag{10}$$

where all terms can be clearly identified; first equation represents the dynamic equilibrium of the elastic substructures, second equation imposes the interface constraint condition between the substructure boundaries and the frame, and last equation imposes the frame equilibrium condition.

We note that the above equation set, when specialized to finite element formulation, may be traced to the form of *hybrid* finite-element models [4].

Implicit integration in time of the displacements $\mathbf{u}$ by the Newmark method, gives the following relations

$$\begin{cases} \mathbf{u}^{n+1} = \mathbf{u}^n + \Delta t \dot{\mathbf{u}}^n + \Delta t^2 \left\{ \left(\frac{1}{2} - \beta \right) \ddot{\mathbf{u}}^n + \beta \ddot{\mathbf{u}}^{n+1} \right\} \\ \dot{\mathbf{u}}^{n+1} = \dot{\mathbf{u}}^n + \Delta t \left\{ (1-\gamma) \ddot{\mathbf{u}}^n + \gamma \ddot{\mathbf{u}}^{n+1} \right\} \end{cases} \tag{11}$$

where n and $n+1$ denote the current and next time step index, respectively, $\Delta t = t^{n+1} - t^n$ the time-step size, while β and γ are time integration parameters that determine stability and accuracy characteristics.

Suppose that computations using this method have successfully proceeded until $t = t^n$ so we know $\mathbf{u}^n$, $\dot{\mathbf{u}}^n$ and $\ddot{\mathbf{u}}^n$. Substitution of the Newmark approximation (11) into the first equation of system (10) and moving next-step accelerations to the left-hand side, leads to the following set of equations:

$$\begin{bmatrix} \mathbf{K}_d & \mathbf{B} & \mathbf{0} \\ \mathbf{B}^\mathsf{T} & \mathbf{0} & -\mathbf{L}_f \\ \mathbf{0} & -\mathbf{L}_f^\mathsf{T} & \mathbf{0} \end{bmatrix} \begin{Bmatrix} \ddot{\mathbf{u}} \\ \boldsymbol{\lambda} \\ \ddot{\mathbf{u}}_f \end{Bmatrix}^{n+1} = \begin{Bmatrix} \mathbf{g}_u \\ \mathbf{0} \\ \mathbf{0} \end{Bmatrix}^{n+1} \tag{12}$$

in which

$$\mathbf{K}_d = \mathbf{M} + \beta \Delta t^2 \mathbf{K}, \quad \mathbf{g}_u^{n+1} = \mathbf{f}^{n+1} - \mathbf{K} \left\{ \mathbf{u}^n + \Delta t \dot{\mathbf{u}}^n + \Delta t^2 \left(\frac{1}{2} - \beta \right) \ddot{\mathbf{u}}^n \right\} \tag{13}$$

are the assembled discrete dynamic masses and equivalent forces.

In a final step, eliminating the substructure accelerations $\ddot{\mathbf{u}}^{n+1}$ from the first equation, we arrive to the classical flexibility form of the AFETI method:

$$\begin{bmatrix} \mathbf{F}_{bb} & \mathbf{L}_f \\ \mathbf{L}_f^\mathsf{T} & \mathbf{0} \end{bmatrix} \begin{Bmatrix} \boldsymbol{\lambda} \\ \ddot{\mathbf{u}}_f \end{Bmatrix}^{n+1} = \begin{Bmatrix} \mathbf{b}_\lambda \\ \mathbf{0} \end{Bmatrix}^{n+1} \tag{14}$$

where the boundary flexibility matrix and the free-term vector are given by the expressions

$$\mathbf{F}_{bb} = \mathbf{B}^\mathsf{T} \mathbf{K}_d^{-1} \mathbf{B}, \quad \mathbf{b}_\lambda^{n+1} = \mathbf{B}^\mathsf{T} \mathbf{K}_d^{-1} \mathbf{g}_u^{n+1} \tag{15}$$

This is a saddle-point problem that can be solved using the classical methodology described in Appendix A.1 that we will denominate here AFETI-B (Basic). For that purpose, we need to introduce here the *projector* concept.

In general, a projector is a linear operator constructed using two different matrices; matrix $\mathbf{B} \in \mathbb{R}^{n \times m}$

with $m < n$ and a symmetric matrix $\mathbf{A} \in \mathbb{R}^{n \times n}$ such that $\mathbf{B}^{\mathsf{T}}\mathbf{A}\mathbf{B}$ is positive definite. Then, the projector $\mathcal{P}_{\mathbf{B}}^{\mathbf{A}}$ is obtained using the following systematic definition:

$$\mathcal{P}_{\mathbf{B}}^{\mathbf{A}} = \mathbf{I} - \mathbf{A}\mathbf{B}\left[\mathbf{B}^{\mathsf{T}}\mathbf{A}\mathbf{B}\right]^{-1}\mathbf{B}^{\mathsf{T}} \tag{16}$$

satisfying the basic conditions $\mathcal{P}_{\mathbf{B}}^{\mathbf{A}}\mathbf{A}\mathbf{B} = \mathbf{0}$ and $\mathbf{B}^{\mathsf{T}}\mathcal{P}_{\mathbf{B}}^{\mathbf{A}} = \mathbf{0}$. When matrix $\mathbf{A}$ is not indicated, it is assumed to be the identity matrix, i.e., $\mathbf{A} = \mathbf{I}$, and the projector becomes symmetric. Recursively, matrix $\mathbf{A}$ itself can be constructed using another projector, giving place to the different levels of projection. A formal definition of the projection concept, together with rules for selecting matrices $\mathbf{A}$ and $\mathbf{B}$ at different levels of projection, is contained in the Appendices.

Hence, we can construct a basic projector $\mathcal{P}_{\mathbf{L}_f}$ using rule (16) and write:

$$\boldsymbol{\lambda} = \mathcal{P}_{\mathbf{L}_f}\boldsymbol{\lambda}_d \tag{17}$$

where $\boldsymbol{\lambda}_d$ is a general vector of localized multipliers, not necessarily in equilibrium, that after filtered by the projector $\mathcal{P}_{\mathbf{L}_f}$ produces a new vector of multipliers $\boldsymbol{\lambda}$ satisfying the frame equilibrium condition $\mathbf{L}_f^{\mathsf{T}}\boldsymbol{\lambda} = \mathbf{0}$.

Substituting the filtered multipliers back in (14), the problem is reduced to a minimization of the residual:

$$\mathbf{r}_\lambda(\boldsymbol{\lambda}) = \mathcal{P}_{\mathbf{L}_f}^{\mathsf{T}}\left\{\mathbf{b}_\lambda - \mathbf{F}_{bb}\boldsymbol{\lambda}\right\} \tag{18}$$

a problem than can be solved iteratively using the iterative PCG process described in Algorithm 1, by simply substituting in the pseudocode $\mathbf{A} = \mathbf{F}_{bb}$ and $\mathcal{P} = \mathcal{P}_{\mathbf{L}_f}$.

Remark 1. The complete expression for $\mathcal{P}_{\mathbf{L}_f}$ is obtained applying the projector definition (16), substituting $\mathbf{A} = \mathbf{I}$ and $\mathbf{B} = \mathbf{L}_f$ to yield:

$$\mathcal{P}_{\mathbf{L}_f} = \mathbf{I} - \mathbf{L}_f\left[\mathbf{L}_f^{\mathsf{T}}\mathbf{L}_f\right]^{-1}\mathbf{L}_f^{\mathsf{T}}.$$

This is the basic multipliers averaging projector of AFETI, hence the name of AFETI-B method. Note that its computation is trivial, because $\left[\mathbf{L}_f^{\mathsf{T}}\mathbf{L}_f\right]$ is a diagonal matrix containing the number of localized multipliers connected to each frame node.

Finally, an efficient iterative solution of (18) requires the use of an adequate preconditioner. For this

Algorithm 1 Preconditioned conjugate-gradient (PCG) algorithm. This algorithm solves for $\mathcal{P}\mathbf{x}$ by minimizing the residual $\mathbf{r}(\mathbf{x}) = \mathcal{P}^{\mathsf{T}}\{\mathbf{b} - \mathbf{A}\mathbf{x}\}$ using the preconditioner $\mathbf{A}^{+}$.

$\mathbf{r}_0 = \mathcal{P}^{\mathsf{T}}\{\mathbf{b} - \mathbf{A}\mathbf{x}_0\}$	▷ Initial projected residual
k=0	▷ Initialize iteration counter
while $\|\mathbf{r}_{k+1}\|/\|\mathbf{r}_0\| > \varepsilon$ **do**	▷ Check convergence
$\mathbf{z}_k = \mathbf{A}^{+}\mathbf{r}_k$	▷ Precondition step
$\mathbf{y}_k = \mathcal{P}\mathbf{z}_k$	▷ Project preconditioned residual
$\beta_k = \frac{\mathbf{y}_k^{\mathsf{T}}\mathbf{r}_k}{\mathbf{y}_{k-1}^{\mathsf{T}}\mathbf{r}_{k-1}}$	▷ Conjugation (for $k = 0$, set $\beta_0 = 0$)
$\mathbf{s}_k = \mathbf{y}_k + \beta_k\mathbf{s}_{k-1}$	▷ Search direction (for $k = 0$, set $\mathbf{s}_0 = \mathbf{y}_0$)
$\mathbf{d}_k = \mathbf{A}\mathbf{s}_k$	▷ Solution step
$\alpha_k = \frac{\mathbf{y}_k^{\mathsf{T}}\mathbf{r}_k}{\mathbf{s}_k^{\mathsf{T}}\mathbf{d}_k}$	▷ Minimization
$\mathbf{x}_{k+1} = \mathbf{x}_k + \alpha_k\mathbf{s}_k$	▷ Update solution
$\mathbf{r}_{k+1} = \mathbf{r}_k - \alpha_k\mathcal{P}^{\mathsf{T}}\mathbf{d}_k$	▷ Update projected residual
$k \leftarrow k + 1$	▷ Increment iteration counter
end while	▷ Repeat until convergence

task, we construct the following approximation to be used as preconditioner,

$$\mathbf{F}_{bb}^{+} = \mathbf{B}^{\mathsf{T}}\mathbf{K}_d\mathbf{B} \tag{19}$$

that is known in the FETI literature as *lumped* preconditioner.

Remark 2. It is well known that the lack of a coarse problem, makes AFETI-B algorithm not scalable. Also, note that the main differences between (14) and the classical FETI-T formulation for transient dynamics, lie in the presence of localized Lagrange multipliers and presence of the interface displacements $\mathbf{u}_f$.

2.2. Partitioned equations of motion with explicit rigid-body modes

The localized partitioned equations of motion (10) have a full rank. However, rank sufficiency is not enough when one solves the equation in a partitioned manner. For example, when a subsystem becomes completely free-free as a result of partitioning, its self-equilibrium state must be part of the solution [42]. The variational infusion of the self-equilibrium states for all the subsystems can be accomplished by decomposing the subsystem total displacements into the deformation states and the self-equilibrium states.

In linear FEM, the floating modes emanate intrinsically from the rank deficiency of the substructural stiffness matrix [50], but can also be directly constructed from simple geometrical considerations [10, 11].

Grouping all the nodal components in a global vector, the total displacements of the substructure can then be separated into a pure deformational component plus a rigid-body part, decomposition that

is written [51]:

$$\mathbf{u} = \mathbf{d} + \mathbf{R}\boldsymbol{\alpha} \tag{20}$$

where $\mathbf{u} \in \mathbb{R}^n$ are the nodal displacements with n the number of DOFs, $\mathbf{d} \in \mathbb{R}^n$ represents the vector of pure-deformational displacements, $\mathbf{R} \in \mathbb{R}^{n \times n_\alpha}$ is a basis of rigid-body modes and vector $\boldsymbol{\alpha} \in \mathbb{R}^{n_\alpha}$ collects the amplitudes of the n_α rigid-body motions.

The variational energy functional derived previously can be further decomposed by dividing the total displacements into deformations and rigid-body motions. This is accomplished by using the projector [46, 20]:

$$\mathcal{P}_{\mathbf{R}}^{\mathbf{M}} = \mathbf{I} - \mathbf{M}\mathbf{R}\mathbf{M}_\alpha^{-1}\mathbf{R}^\mathsf{T} \tag{21}$$

where $\mathbf{M}$ is a symmetric definite positive mass matrix and $\mathbf{M}_\alpha = \mathbf{R}^\mathsf{T}\mathbf{M}\mathbf{R}$ is the principal mass matrix introduced by Park et al. in [40], a (6×6) matrix for a three-dimensional floating substructure. This operator presents the following filtering properties

$$\mathcal{P}_{\mathbf{R}}^{\mathbf{M}^\mathsf{T}}\mathbf{R} = \mathbf{0}, \quad \mathcal{P}_{\mathbf{R}}^{\mathbf{M}}\mathbf{M}\mathbf{R} = \mathbf{0} \tag{22}$$

allowing to separate pure deformational modes from rigid-body motions using the following expressions:

$$\mathbf{d} = \mathcal{P}_{\mathbf{R}}^{\mathbf{M}^\mathsf{T}}\mathbf{u}, \quad \mathbf{R}\boldsymbol{\alpha} = (\mathbf{I} - \mathcal{P}_{\mathbf{R}}^{\mathbf{M}^\mathsf{T}})\mathbf{u} \tag{23}$$

where, by definition, the projector $\mathcal{P}_{\mathbf{R}}^{\mathbf{M}^\mathsf{T}} \in \mathbb{R}^{n \times n}$ performs an orthogonal projection in the subspace defined by the rigid-body modes and therefore is acting as a filter for the deformational component of displacements.

Grouping all the nodal components in a global vector, the total displacements of the substructure can then be separated into a pure deformational component plus a rigid-body part, decomposition that is written

$$\mathbf{u} = \mathcal{P}_{\mathbf{R}}^{\mathbf{M}^\mathsf{T}}\mathbf{d} + \mathbf{R}\boldsymbol{\alpha} \tag{24}$$

where $\mathbf{d}^\mathsf{T} = \left[\mathbf{d}_1^\mathsf{T} \cdots \mathbf{d}_N^\mathsf{T}\right]$ is the partitioned subsystem-by-subsystem deformational displacement vector and $\boldsymbol{\alpha}^\mathsf{T} = \left[\boldsymbol{\alpha}_1^\mathsf{T} \cdots \boldsymbol{\alpha}_N^\mathsf{T}\right]$ groups the amplitudes which multiply substructural RBMs.

In particular, for a system partitioned into N subsystems, the matrices in (24) take the following

block-diagonal form:

$$\mathcal{P}_{\mathbf{R}}^{\mathbf{M}} = \begin{bmatrix} \mathcal{P}_{\mathbf{R}_1}^{\mathbf{M}_1} & \cdots & \mathbf{0} \\ \vdots & \ddots & \vdots \\ \mathbf{0} & \cdots & \mathcal{P}_{\mathbf{R}_N}^{\mathbf{M}_N} \end{bmatrix}, \quad \mathbf{R} = \begin{bmatrix} \mathbf{R}_1 & \cdots & \mathbf{0} \\ \vdots & \ddots & \vdots \\ \mathbf{0} & \cdots & \mathbf{R}_N \end{bmatrix}$$

with each diagonal entry affecting their corresponding amplitudes $\mathbf{d}_i$ and $\boldsymbol{\alpha}_i$, respectively. Substructural modes $\mathbf{R}_i$ are defined through the following orthogonality property:

$$\mathbf{K}_i\mathbf{R}_i \;=\; \mathbf{0} \qquad (i = 1 \ldots N). \tag{25}$$

Substituting displacement decomposition (24) into the variational form (9), leads to:

$$\delta\mathscr{W}_t\left(\mathbf{d}, \boldsymbol{\alpha}, \mathbf{u}_f, \boldsymbol{\lambda}\right) = \delta\left(\mathbf{d}^{\mathsf{T}}\mathcal{P}_{\mathbf{R}}^{\mathbf{M}} + \boldsymbol{\alpha}^{\mathsf{T}}\mathbf{R}^{\mathsf{T}}\right)\left\{\mathbf{M}\left(\mathcal{P}_{\mathbf{R}}^{\mathbf{M}^{\mathsf{T}}}\ddot{\mathbf{d}} + \mathbf{R}\ddot{\boldsymbol{\alpha}}\right) + \mathbf{K}\left(\mathcal{P}_{\mathbf{R}}^{\mathbf{M}^{\mathsf{T}}}\mathbf{d} + \mathbf{R}\boldsymbol{\alpha}\right) - \mathbf{f}\right\} + \delta\left\{\boldsymbol{\lambda}^{\mathsf{T}}\left(\mathbf{B}^{\mathsf{T}}\left(\mathcal{P}_{\mathbf{R}}^{\mathbf{M}^{\mathsf{T}}}\mathbf{d} + \mathbf{R}\boldsymbol{\alpha}\right) - \mathbf{L}_f\mathbf{u}_f\right)\right\} \tag{26}$$

an equivalent variational form expressed in terms of deformational and rigid body displacements.

Exploiting the mass-orthogonality between the deformational and rigid body modes (22) and substituting (25), the stationarity condition $\delta\mathscr{W}_t = 0$ of equation (26) yields the following four-variable partitioned equations of motion:

$$\begin{bmatrix} \mathbf{K} + \bar{\mathbf{M}}\frac{d^2}{dt^2} & \mathbf{0} & \mathbf{B}_d & \mathbf{0} \\ \mathbf{0} & \mathbf{M}_\alpha\frac{d^2}{dt^2} & \mathbf{R}_b^{\mathsf{T}} & \mathbf{0} \\ \mathbf{B}_d^{\mathsf{T}} & \mathbf{R}_b & \mathbf{0} & -\mathbf{L}_f \\ \mathbf{0} & \mathbf{0} & -\mathbf{L}_f^{\mathsf{T}} & \mathbf{0} \end{bmatrix} \begin{Bmatrix} \mathbf{d} \\ \boldsymbol{\alpha} \\ \boldsymbol{\lambda} \\ \mathbf{u}_f \end{Bmatrix} = \begin{Bmatrix} \mathbf{f}_d \\ \mathbf{f}_\alpha \\ \mathbf{0} \\ \mathbf{0} \end{Bmatrix} \tag{27}$$

with the following definitions

$$\bar{\mathbf{M}} = \mathcal{P}_{\mathbf{R}}^{\mathbf{M}}\mathbf{M}\mathcal{P}_{\mathbf{R}}^{\mathbf{M}^{\mathsf{T}}} = \mathcal{P}_{\mathbf{R}}^{\mathbf{M}}\mathbf{M}, \quad \mathbf{B}_d = \mathcal{P}_{\mathbf{R}}^{\mathbf{M}}\mathbf{B}, \quad \mathbf{R}_b = \mathbf{B}^{\mathsf{T}}\mathbf{R}, \quad \mathbf{f}_d = \mathcal{P}_{\mathbf{R}}^{\mathbf{M}}\mathbf{f}, \quad \mathbf{f}_\alpha = \mathbf{R}^{\mathsf{T}}\mathbf{f} \tag{28}$$

where all terms can be clearly identified; first equation represents the equilibrium of the deformational part of the FEM elastic equations, second equation is the rigid-body dynamic equilibrium condition, third equation imposes the interface constraint condition between the substructure boundary and the frame and last equation imposes the frame equilibrium condition.

Equation (27) consists of coupled four-variable partitioned equations. The first row represents the

equations of motion for the deformable modes for each of the partitioned subsystems; the second is *d'Alembert's* principal equation for each of the partitioned subsystems; the third is the interface kinematical constraints; and, the fourth is the Newton's third law along the interfaces in terms of localized Lagrange multipliers.

This means that the three variables $(\mathbf{d}, \boldsymbol{\alpha}, \boldsymbol{\lambda})$ are localized. It is the frame displacement $\mathbf{u}_f$ that connects the interfaces of partitioned subsystems.

To obtain the time discrete equations, suppose computations have proceeded until $t = t^n$. Substitution of Newmark time integration scheme (11) into the first and second equation of (27) and moving next-step accelerations to the left-hand side, leads to the following set of discrete equations:

$$\begin{bmatrix} \bar{\mathbf{K}}_d & \mathbf{0} & \mathbf{B}_d & \mathbf{0} \\ \mathbf{0} & \mathbf{M}_\alpha & \mathbf{R}_b^\mathsf{T} & \mathbf{0} \\ \mathbf{B}_d^\mathsf{T} & \mathbf{R}_b & \mathbf{0} & -\mathbf{L}_f \\ \mathbf{0} & \mathbf{0} & -\mathbf{L}_f^\mathsf{T} & \mathbf{0} \end{bmatrix} \begin{Bmatrix} \ddot{\mathbf{d}} \\ \ddot{\boldsymbol{\alpha}} \\ \boldsymbol{\lambda} \\ \ddot{\mathbf{u}}_f \end{Bmatrix}^{n+1} = \begin{Bmatrix} \mathbf{g}_d \\ \mathbf{f}_\alpha \\ \mathbf{0} \\ \mathbf{0} \end{Bmatrix}^{n+1} \tag{29}$$

with separated deformational and rigid body accelerations, in which:

$$\bar{\mathbf{K}}_d = \bar{\mathbf{M}} + \beta \Delta t^2 \mathbf{K}, \quad \mathbf{g}_d^{n+1} = \mathcal{P}_{\mathbf{R}}^{\mathbf{M}} \mathbf{g}_u^{n+1} \tag{30}$$

and where we have replaced the fourth equation of (27) by its twice time-differentiated expression.

Since $\bar{\mathbf{K}}_d = \mathbf{K}_d \mathcal{P}_{\mathbf{R}}^{\mathbf{M}^\mathsf{T}}$ and using the idempotent property of the projector, deformational accelerations can be isolated from the first equation of (29):

$$\mathcal{P}_{\mathbf{R}}^{\mathbf{M}^\mathsf{T}} \ddot{\mathbf{d}}^{n+1} = \bar{\mathbf{F}} (\mathbf{g}_u^{n+1} - \mathbf{B} \boldsymbol{\lambda}^{n+1}) \tag{31}$$

where $\bar{\mathbf{F}}$ is the projected dynamic flexibility matrix, that can be expressed as:

$$\bar{\mathbf{F}} = \mathcal{P}_{\mathbf{R}}^{\mathbf{M}^\mathsf{T}} \mathbf{K}_d^{-1} \mathcal{P}_{\mathbf{R}}^{\mathbf{M}} = \mathbf{K}_d^{-1} - \mathbf{R} \mathbf{M}_\alpha^{-1} \mathbf{R}^T \tag{32}$$

a relation that is demonstrated in [20].

Now, eliminating $\ddot{\mathbf{d}}^{n+1}$ from (29) yields the following three-variable difference equation set:

$$\begin{bmatrix} \bar{\mathbf{F}}_{bb} & -\mathbf{R}_b & \mathbf{L}_f \\ -\mathbf{R}_b^{\mathsf{T}} & -\mathbf{M}_\alpha & \mathbf{0} \\ \mathbf{L}_f^{\mathsf{T}} & \mathbf{0} & \mathbf{0} \end{bmatrix} \begin{Bmatrix} \boldsymbol{\lambda} \\ \ddot{\boldsymbol{\alpha}} \\ \ddot{\mathbf{u}}_f \end{Bmatrix}^{n+1} = \begin{Bmatrix} \bar{\mathbf{b}}_\lambda \\ -\mathbf{f}_\alpha \\ \mathbf{0} \end{Bmatrix}^{n+1} \tag{33}$$

with

$$\bar{\mathbf{F}}_{bb} = \mathbf{B}^{\mathsf{T}}\bar{\mathbf{F}}\mathbf{B} = \mathbf{F}_{bb} - \mathbf{R}_b\mathbf{M}_\alpha^{-1}\mathbf{R}_b^{\mathsf{T}}, \quad \bar{\mathbf{b}}_\lambda^{n+1} = \mathbf{b}_\lambda^{n+1} - \mathbf{R}_b\mathbf{M}_\alpha^{-1}\mathbf{f}_\alpha \tag{34}$$

which will be called as the *basic dual-primal partitioned equations of motion*. This equation will serve as the basis from which we will develop a series of partitioned solution algorithms that are applicable both for static and dynamic problems.

This partitioned flexibility system represents the *basic dual-primal partitioned equations of motion* with localized Lagrange multipliers, first proposed by Park et. al. for statics [12, 15, 14], generalized to structural dynamics by Gumaste et al. [13] and later extended to multi-body dynamics with large rotations [20].

Remark 3. Time-integration stability of partitioned systems with localized Lagrange multipliers has been studied by Ross et al. [16] for different time integration schemes, demonstrating that partitioning does not affect the A-stability condition of the Newmark method, obtained with $\gamma \geq 1/2$ and $\beta \geq \gamma/2$, whereas global second order accuracy is achieved for $\gamma = 1/2$.

3. Review of existent AFETI algorithms for dynamics

In this section we summarize existent AFETI methods for the solution of the dynamic partitioned equations of motion. We will focus here on fully implicit solution algorithms, explicit-implicit methods for the AFETI dynamic equations were previously studied in [46].

3.1. Implicit solution algorithm AFETI-I without coarse problem

From a historical perspective, first parallel solution algorithms in the context of AFETI methods in dynamics were proposed by Gumaste et al. [13]. In this section, our intention is to introduce that formulation by adding some minor changes to the parallel implicit dynamic solution method initially proposed. This implicit scheme is based on a straight iterative solution of system (33) using PCG algorithm, a technique that can be simplified introducing the following modifications:

1. Project the interface Lagrange multipliers using the filter $\mathcal{P}_{\mathbf{L}_f}$ to automatically satisfy the frame equilibrium condition.

2. Solve for the substructure-by-substructure global multipliers $\boldsymbol{\lambda}_\alpha = \mathbf{R}_b^\mathsf{T}\mathcal{P}_{\mathbf{L}_f}\boldsymbol{\lambda}$ instead of solving for the rigid body accelerations $\ddot{\boldsymbol{\alpha}}$, performing the change of variable,

$$\ddot{\boldsymbol{\alpha}} = \mathbf{M}_\alpha^{-1}\left\{\mathbf{f}_\alpha - \boldsymbol{\lambda}_\alpha\right\}. \tag{35}$$

After introducing these modifications in (33) and performing the time discretization, we obtain a new system where the vector of unknowns is composed only by the localized and global multipliers,

$$\begin{bmatrix} \mathcal{P}_{\mathbf{L}_f}^\mathsf{T}\bar{\mathbf{F}}_{bb}\mathcal{P}_{\mathbf{L}_f} & \mathcal{P}_{\mathbf{L}_f}^\mathsf{T}\mathbf{R}_b\mathbf{M}_\alpha^{-1} \\ \mathbf{M}_\alpha^{-1}\mathbf{R}_b^\mathsf{T}\mathcal{P}_{L_f} & -\mathbf{M}_\alpha^{-1} \end{bmatrix} \begin{Bmatrix} \boldsymbol{\lambda} \\ \boldsymbol{\lambda}_\alpha \end{Bmatrix}^{n+1} = \begin{Bmatrix} \mathcal{P}_{\mathbf{L}_f}^\mathsf{T}\mathbf{b}_\lambda \\ \mathbf{0} \end{Bmatrix}^{n+1} \tag{36}$$

which can be solved using the PCG solution algorithm combined with an appropriated preconditioner. A generalized inverse of block matrices with an structure like the one present in the left-hand side of (36) can be found in [52], from where we construct the following approximation to be used as preconditioner,

$$\mathbf{S}^+ = \begin{bmatrix} \hat{\mathbf{F}}_{bb}^+ & -\hat{\mathbf{F}}_{bb}^+\mathbf{R}_b \\ -\mathbf{R}_b^\mathsf{T}\hat{\mathbf{F}}_{bb}^+ & -\mathbf{M}_\alpha + \mathbf{R}_b^\mathsf{T}\mathcal{P}_{\mathbf{L}_f}\hat{\mathbf{F}}_{bb}^+\mathcal{P}_{\mathbf{L}_f}^\mathsf{T}\mathbf{R}_b \end{bmatrix} \tag{37}$$

where $\hat{\mathbf{F}}_{bb}^+$ is also an approximation to the generalized inverse of $\mathcal{P}_{\mathbf{L}_f}^\mathsf{T}\bar{\mathbf{F}}_{bb}\mathcal{P}_{\mathbf{L}_f}$ defined as

$$\hat{\mathbf{F}}_{bb}^+ = \mathcal{P}_{\mathbf{L}_f}^\mathsf{T}\bar{\mathbf{K}}_{bb}\mathcal{P}_{\mathbf{L}_f} \approx \left[\mathcal{P}_{\mathbf{L}_f}^\mathsf{T}\bar{\mathbf{F}}_{bb}\mathcal{P}_{\mathbf{L}_f}\right]^+ \tag{38}$$

Remark 4. Although this solution method is simple, it was demonstrated in [13] that it utilizes no coarse solver, hence its performance is comparable to the AFETI-B dynamic algorithm. However, important convergence improvements were obtained in the same reference using a flexibility normalization technique with infusion of substructural deformation modes.

3.2. Explicit-implicit solution algorithm AFETI-EI with coarse problem

This algorithm transforms the transient problem in an equivalent static problem with explicitly predicted inertia forces [46].

From inspection of system (33) together with previous considerations, it is deduced that the only thing we need to proceed with a dynamic analysis using the classical AFETI algorithm designed for static problems, is a good approximation of the substructure-by-substructure rigid body accelerations $\ddot{\boldsymbol{\alpha}}_p^{n+1}$ to construct a prediction of the global multipliers $\boldsymbol{\lambda}_\alpha^p = \mathbf{f}_\alpha^{n+1} - \mathbf{M}_\alpha\ddot{\boldsymbol{\alpha}}_p^{n+1}$ and simplify the second

row of the system. The system adopts then the classical AFETI form:

$$\begin{bmatrix} \bar{\mathbf{F}}_{bb} & -\mathbf{R}_b & \mathbf{L}_f \\ -\mathbf{R}_b^{\mathsf{T}} & \mathbf{0} & \mathbf{0} \\ \mathbf{L}_f^{\mathsf{T}} & \mathbf{0} & \mathbf{0} \end{bmatrix} \begin{Bmatrix} \boldsymbol{\lambda} \\ \ddot{\boldsymbol{\alpha}} \\ \ddot{\mathbf{u}}_f \end{Bmatrix}^{n+1} = \begin{Bmatrix} \bar{\mathbf{b}}_\lambda \\ -\boldsymbol{\lambda}_\alpha^p \\ \mathbf{0} \end{Bmatrix}^{n+1} \tag{39}$$

that can be solved using efficient AFETI algorithms for statics available in the literature [53].

This way, we have transformed a dynamic problem into an equivalent static problem and now the same solver can be used for statics and dynamics. The simplest projector to solve this problem, thus the slowest to converge, is:

$$\boldsymbol{\lambda} = \mathcal{P}_{\mathbf{L}_f}^{\mathcal{P}_{\mathbf{R}_b}} \left\{ \mathcal{P}_{\mathbf{R}_b} \boldsymbol{\lambda}_d + \mathbf{R}_b \boldsymbol{\lambda}_r \right\} \tag{40}$$

decomposition employed in the original development of the AFETI method [10, 11]. Although this decomposition is very effective, it has the inconvenience that the size of its coarse problem is equal to the size of the interface. Another method, based on decomposition (C.8), was proposed by Gumaste et al. [13] using the following projection:

$$\boldsymbol{\lambda} = \mathcal{P}_{\mathbf{L}_f} \left\{ \mathcal{P}_{\mathbf{R}_b}^{\mathcal{P}_{\mathbf{L}_f}^{\mathsf{T}}} \boldsymbol{\lambda}_d + \mathbf{R}_b \boldsymbol{\lambda}_r \right\} \tag{41}$$

a better option than decomposition (40), because the size of the coarse problem is now equal to the number of rigid-body modes and it is also simpler to evaluate.

After introducing decomposition (41) into the system (39), we can solve iteratively for the deformational part of the multipliers $\boldsymbol{\lambda}_d$, by using Algorithm 1 to minimize the residual:

$$\mathbf{r}_\lambda^{\mathrm{S}}(\boldsymbol{\lambda}) = \mathcal{P}_{\mathbf{R}_b}^{\mathcal{P}_{\mathbf{L}_f}} \mathcal{P}_{\mathbf{L}_f}^{\mathsf{T}} \left\{ \bar{\mathbf{b}}_\lambda - \bar{\mathbf{F}}_{bb} \boldsymbol{\lambda} \right\} \tag{42}$$

satisfying by design the condition $\mathbf{R}_b^{\mathsf{T}} \mathbf{r}_\lambda^{\mathrm{S}}(\boldsymbol{\lambda}) = \mathbf{0}$, thanks to the projector that repeatedly enforces global static equilibrium at each iteration. The problem with this approach is the accumulation of errors in time, due to prediction of the substructural net multipliers $\boldsymbol{\lambda}_\alpha^p$, requiring the use of extra correction steps to maintain accuracy and stability [46].

4. AFETI dynamic solution algorithms with projection

The weakness of the solution algorithms mentioned in Section 3, reside in the absence of a natural projector capable of enforcing at the same time, the equilibrium of the localized Lagrange multipliers

and the dynamic global equilibrium of the substructures. In this Section we propose natural projectors that satisfy both requirements.

The first one is inspired by the classical FETI-T decomposition of Lagrange multipliers proposed by Farhat et al. [23, 24] in the context of FETI methods for dynamic problems. The second algorithm represents a natural extension to second level decompositions. Some discussion about the benefits and drawbacks of each solution method is included.

4.1. One-level projection - AFETI-1

In this section we develop an AFETI algorithm for dynamics equivalent to the classical FETI-T method proposed by Farhat et al. for classical Lagrange multipliers, that supposes a generalization to the case of localized Lagrange multipliers. As in the case of classical Lagrange multipliers, the advantage of this new method will be the presence of a coarse problem that makes the problem numerically scalable for second order elasticity problems. By analogy with the FETI-T method, this new method will be named *AFETI-1 method with coarse problem*. AFETI-1 can be considered as a localized version of the FETI-T method.

We propose a one-level decomposition of the localized multipliers of the form (C.8):

$$\boldsymbol{\lambda} = \mathcal{P}_{\mathbf{L}_f} \left\{ \mathcal{P}_{\mathbf{R}_b}^{\boldsymbol{\Psi}\ \mathsf{T}} \boldsymbol{\lambda}_d + \mathbf{R}_b \boldsymbol{\lambda}_r \right\} \tag{43}$$

with $\boldsymbol{\Psi} = \mathcal{P}_{\mathbf{L}_f}^{\mathsf{T}} \mathbf{F}_{bb} \mathcal{P}_{\mathbf{L}_f}$, a projection that combined with system (14) yields the following decoupled equation set:

$$\begin{bmatrix} \mathcal{P}_{\mathbf{R}_b}^{\boldsymbol{\Psi}} \boldsymbol{\Psi} \mathcal{P}_{\mathbf{R}_b}^{\boldsymbol{\Psi}\ \mathsf{T}} & \mathbf{0} \\ \mathbf{0} & \mathbf{R}_b^{\mathsf{T}} \boldsymbol{\Psi} \mathbf{R}_b \end{bmatrix} \begin{Bmatrix} \boldsymbol{\lambda}_d \\ \boldsymbol{\lambda}_r \end{Bmatrix}^{n+1} = \begin{Bmatrix} \mathcal{P}_{\mathbf{R}_b}^{\boldsymbol{\Psi}} \mathcal{P}_{\mathbf{L}_f}^{\mathsf{T}} \mathbf{b}_\lambda^{n+1} \\ \mathbf{R}_b^{\mathsf{T}} \mathcal{P}_{\mathbf{L}_f}^{\mathsf{T}} \mathbf{b}_\lambda^{n+1} \end{Bmatrix} \tag{44}$$

that is associated with a new projected residual given by

$$\mathbf{r}_\lambda^{\mathrm{D1}} (\boldsymbol{\lambda}) = \mathcal{P}_{\mathbf{R}_b}^{\boldsymbol{\Psi}} \mathcal{P}_{\mathbf{L}_f}^{\mathsf{T}} \left\{ \mathbf{b}_\lambda - \mathbf{F}_{bb} \boldsymbol{\lambda} \right\} \tag{45}$$

and can be solved iteratively through PCG Algorithm 1 with projector $\mathcal{P} = \mathcal{P}_{\mathbf{L}_f} \mathcal{P}_{\mathbf{R}_b}^{\boldsymbol{\Psi}\ \mathsf{T}}$.

This new residual is related with (18) by the following projection:

$$\mathbf{r}_\lambda^{\mathrm{D1}} (\boldsymbol{\lambda}) = \mathcal{P}_{\mathbf{R}_b}^{\boldsymbol{\Psi}} \mathbf{r}_\lambda (\boldsymbol{\lambda}) \tag{46}$$

where the projector $\mathcal{P}_{\mathbf{R}_b}^{\boldsymbol{\Psi}}$ introduces a new coarse problem of the form $\left[\mathbf{R}_b^{\mathsf{T}} \boldsymbol{\Psi} \mathbf{R}_b \right] \mathbf{x} = \mathbf{b}$ that has to be solved at the projection step of each iteration during the solution process.

Note that $\boldsymbol{\lambda}_r$ in decomposition (43) does not represent the substructure-by-substructure global multipliers, because $\mathbf{R}_b^\mathsf{T}\boldsymbol{\lambda} \neq \boldsymbol{\lambda}_r$. However, the following equality holds $\mathbf{R}_b^\mathsf{T}\mathcal{P}_{\mathbf{L}_f}^\mathsf{T}\mathbf{F}_{bb}\boldsymbol{\lambda} = \mathbf{R}_b^\mathsf{T}\boldsymbol{\Psi}\mathbf{R}_b\boldsymbol{\lambda}_r$.

Remark 5. This algorithm can be considered as a localized version of the FETI-T algorithm, inheriting its basic properties and characteristics. Among them the numerical scalability for second order elasticity problems, that is recovered thanks to the introduction of the new coarse problem given by the global equilibrium equation.

Remark 6. Finally, note that the coarse problem $\left[\mathbf{R}_b^\mathsf{T}\boldsymbol{\Psi}\mathbf{R}_b\right]\mathbf{x} = \mathbf{b}$ introduced by this algorithm depends on the time-step size Δt through the dynamic flexibility matrix $\mathbf{F}_{bb}$. Hence, when time-step changes during the solution process a new orthogonalization of the coarse problem is required. Also note that solving the coarse problem requires inter-process communication.

4.2. Two-level projection - AFETI-2

Now, we extend the space of rigid body motions $\mathbf{R}$ with an orthogonal subspace of deformational displacements $\mathbf{C}$ and extract the boundary components, computed as $\mathbf{B}^\mathsf{T}\left[\mathbf{R}|\mathbf{C}\right] = \left[\mathbf{R}_b|\mathbf{C}_b\right]$, to construct two different subspaces. These separated subspaces are then used to expand the localized Lagrange multipliers by using a two-level decomposition like (C.9) in the form:

$$\boldsymbol{\lambda} = \mathcal{P}_{\mathbf{L}_f}\left\{\mathcal{P}_{\mathbf{R}_b}^{\boldsymbol{\Psi}\,\mathsf{T}}\left(\mathcal{P}_{\mathbf{C}_b}^{\boldsymbol{\Omega}\,\mathsf{T}}\boldsymbol{\lambda}_d + \mathbf{C}_b\boldsymbol{\lambda}_c\right) + \mathbf{R}_b\boldsymbol{\lambda}_r\right\} \tag{47}$$

with matrices $\boldsymbol{\Psi} = \mathcal{P}_{\mathbf{L}_f}^\mathsf{T}\mathbf{F}_{bb}\mathcal{P}_{\mathbf{L}_f}$ and $\boldsymbol{\Omega} = \mathcal{P}_{\mathbf{R}_b}^{\boldsymbol{\Psi}}\boldsymbol{\Psi}\mathcal{P}_{\mathbf{R}_b}^{\boldsymbol{\Psi}\,\mathsf{T}}$. This is a second level projection that, introduced in system (14) and using the new projector properties, yields the following equation set:

$$\begin{bmatrix} \mathcal{P}_{\mathbf{C}_b}^{\boldsymbol{\Omega}}\boldsymbol{\Omega}\mathcal{P}_{\mathbf{C}_b}^{\boldsymbol{\Omega}\,\mathsf{T}} & \mathbf{0} & \mathbf{0} \\ \mathbf{0} & \mathbf{C}_b^\mathsf{T}\mathcal{P}_{\mathbf{R}_b}^{\boldsymbol{\Psi}}\boldsymbol{\Psi}\mathcal{P}_{\mathbf{R}_b}^{\boldsymbol{\Psi}\,\mathsf{T}}\mathbf{C}_b & \mathbf{0} \\ \mathbf{0} & \mathbf{0} & \mathbf{R}_b^\mathsf{T}\boldsymbol{\Psi}\mathbf{R}_b \end{bmatrix}\begin{Bmatrix} \boldsymbol{\lambda}_d \\ \boldsymbol{\lambda}_c \\ \boldsymbol{\lambda}_r \end{Bmatrix}^{n+1} = \begin{Bmatrix} \mathcal{P}_{\mathbf{C}_b}^{\boldsymbol{\Omega}}\mathcal{P}_{\mathbf{R}_b}^{\boldsymbol{\Psi}}\mathcal{P}_{\mathbf{L}_f}^\mathsf{T}\mathbf{b}_\lambda^{n+1} \\ \mathbf{C}_b^\mathsf{T}\mathcal{P}_{\mathbf{R}_b}^{\boldsymbol{\Psi}}\mathcal{P}_{\mathbf{L}_f}^\mathsf{T}\mathbf{b}_\lambda^{n+1} \\ \mathbf{R}_b^\mathsf{T}\mathcal{P}_{\mathbf{L}_f}^\mathsf{T}\mathbf{b}_\lambda^{n+1} \end{Bmatrix} \tag{48}$$

where the three solutions are now completely decoupled. This system is associated with a new two-level projected residual:

$$\mathbf{r}_\lambda^{\mathrm{D}2}\left(\boldsymbol{\lambda}\right) = \mathcal{P}_{\mathbf{C}_b}^{\boldsymbol{\Omega}}\mathbf{r}_\lambda^{\mathrm{D}1}\left(\boldsymbol{\lambda}\right) \tag{49}$$

that can be simply expressed as a projection of the previous one-level residual (45). Note that this residual satisfies two different constraints, i.e., $\mathbf{R}_b^\mathsf{T}\mathbf{r}_\lambda^{\mathrm{D}2} = \mathbf{0}$ and $\mathbf{C}_b^\mathsf{T}\mathbf{r}_\lambda^{\mathrm{D}2} = \mathbf{0}$, thanks to properties (C.3) and (C.4) of the second level AFETI projectors. Therefore, this algorithm is capable of separating the rigid-body equilibrium constraints from the additional deformational constraints.

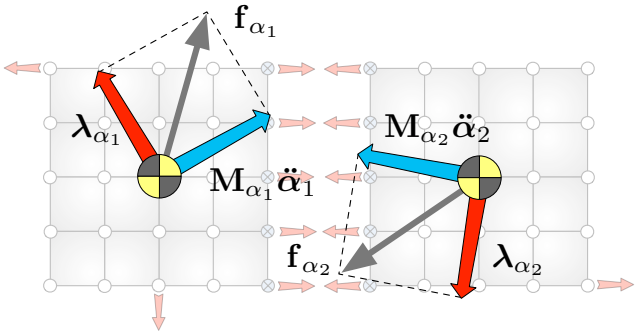

Figure 2: Illustration of the physical interpretation of the d'Alembert-Lagrange balance equations as a substructure-by-substructure net equilibrium condition for the individual partitions.

When it comes to implementation, the component $\mathcal{P}\boldsymbol{\lambda}_d$ of decomposition (47), with the two-level projector $\mathcal{P} = \mathcal{P}_{\mathbf{L}_f}\mathcal{P}_{\mathbf{R}_b}^{\boldsymbol{\Psi}\,\mathsf{T}}\mathcal{P}_{\mathbf{C}_b}^{\boldsymbol{\Omega}\,\mathsf{T}}$, can be computed iteratively using PCG Algorithm 1. This separated decomposition reduces the size of the coarse problem with respect to AFETI-C, to be described later, because extra constraints are introduced through an additional projection. However, upon a close examination of projector $\mathcal{P}_{\mathbf{C}_b}^{\boldsymbol{\Omega}}$, we observe that its construction can be extremely expensive for numerical purposes.

In Section 6, we will propose a new method named AFETI-C that is able to enforce the same constraints to the residual without the need of constructing expensive projectors.

5. Significance of the d'Alembert-Lagrange balance equations

The second equation of (27) represents the self-equilibrium equations of the partitions or *d'Alembert-Lagrange principal equation*, that describes the floating rigid motions [40]. This equation can be written for the floating substructures in the form:

$$\boldsymbol{\lambda}_\alpha^{n+1} + \mathbf{M}_\alpha \ddot{\boldsymbol{\alpha}}^{n+1} = \mathbf{f}_\alpha^{n+1} \tag{50}$$

where $\mathbf{f}_\alpha^{n+1} = \mathbf{R}^\mathsf{T}\mathbf{f}^{n+1}$, defined in (28), represents the net external forces, $\mathbf{M}_\alpha\ddot{\boldsymbol{\alpha}}^{n+1}$ are the global inertia forces and $\boldsymbol{\lambda}_\alpha^{n+1} = \mathbf{R}_b^\mathsf{T}\boldsymbol{\lambda}^{n+1}$ are defined as the *d'Alembert* interface forces. This principle is illustrated in Figure 2 as the necessary condition for global dynamic equilibrium in every partition.

Remark 7. The d'Alembert-Lagrange equation represents the substructure-by-substructure dynamic equilibrium condition.The above solvability condition forms a natural coarse problem which can be used to accelerate the convergence of dynamic and quasi-static partitioned problems.

Theorem 1. *From a mechanical point of view, the convergence improvement of the AFETI-1 method observed when driving to zero the projected residual* (46) *using the PCG iterative solution algorithm,*

comes from an enforcement of the substructure-by-substructure global equilibrium at each iteration. This will reduce the search space of the iterative solver only to those solutions fulfilling the global equilibrium condition.

Proof. The proof follows from consideration of the projected residual (45) where projector $\mathcal{P}^{\mathbf{\Psi}}_{\mathbf{R}_b}$ is used to eliminate all the rigid-body components of $\mathbf{r}_\lambda$, making $\mathbf{R}_b^\mathsf{T}\mathbf{r}_\lambda^{\mathrm{D1}} = \mathbf{0}$. In order to gain some insight into what this projection represents, let us solve for the rigid body accelerations $\ddot{\boldsymbol{\alpha}}$ in the first row of (33) to obtain

$$\ddot{\boldsymbol{\alpha}} = \left[\mathbf{R}_b^\mathsf{T}\mathcal{P}_{\mathbf{L}_f}^\mathsf{T}\mathbf{R}_b\right]^{-1}\mathbf{R}_b^\mathsf{T}\mathcal{P}_{\mathbf{L}_f}^\mathsf{T}\left\{\bar{\mathbf{F}}_{bb}\boldsymbol{\lambda} - \bar{\mathbf{b}}_\lambda\right\} \tag{51}$$

and use the definitions of (28) to write

$$-\mathbf{M}_\alpha\ddot{\boldsymbol{\alpha}} - \mathbf{R}_b^\mathsf{T}\boldsymbol{\lambda} + \mathbf{R}^\mathsf{T}\mathbf{f} = \mathbf{M}_\alpha\left[\mathbf{R}_b^\mathsf{T}\mathcal{P}_{\mathbf{L}_f}^\mathsf{T}\mathbf{R}_b\right]^{-1}\mathbf{R}_b^\mathsf{T}\mathbf{r}_\lambda \tag{52}$$

where we can identify the *d'Alembert-Lagrange* principal balance equation [40] on the left, condition for substructure-by-substructure global equilibrium, with an expression for the global disequilibrium on the right. This global disequilibrium force, defined as $\mathbf{f}_\varepsilon = \mathbf{M}_\alpha\left[\mathbf{R}_b^\mathsf{T}\mathcal{P}_{\mathbf{L}_f}^\mathsf{T}\mathbf{R}_b\right]^{-1}\mathbf{R}_b^\mathsf{T}\mathbf{r}_\lambda$, is related with our original residual (18) by the following expression

$$\left[\mathbf{R}_b^\mathsf{T}\mathcal{P}_{\mathbf{L}_f}^\mathsf{T}\mathbf{R}_b\right]\mathbf{M}_\alpha^{-1}\mathbf{f}_\varepsilon = \mathbf{R}_b^\mathsf{T}\mathbf{r}_\lambda \tag{53}$$

showing that the rigid-body components of the residual are related with the substructure-by-substructure global disequilibrium. This disequilibrium is eliminated when the residual $\mathbf{r}_\lambda$ is projected using $\mathcal{P}^{\mathbf{\Psi}}_{\mathbf{R}_b}$ in order to satisfy the condition $\mathbf{R}_b^\mathsf{T}\mathbf{r}_\lambda^{\mathrm{D1}} = \mathbf{0}$. □

6. A new AFETI-C method with constraints

The AFETI-B problem (14), combined with a group of extra constraints of the type $\mathbf{C}_b^\mathsf{T}\mathbf{r}_\lambda = \mathbf{0}$, can be mathematically expressed as the first-order optimality condition for the following equality-constrained quadratic programming problem:

$$\begin{aligned} \underset{\boldsymbol{\lambda}_d}{\text{minimize}} \quad & \tfrac{1}{2}\boldsymbol{\lambda}_d^\mathsf{T}\mathbf{F}_{bb}\boldsymbol{\lambda}_d - \mathbf{b}_\lambda^\mathsf{T}\boldsymbol{\lambda}_d \\ \text{subject to} \quad & \mathbf{C}_b^\mathsf{T}\left(\mathbf{b}_\lambda - \mathbf{F}_{bb}\boldsymbol{\lambda}_d\right) = \mathbf{0} \end{aligned} \tag{54}$$

where the projected multipliers, defined now as $\boldsymbol{\lambda}_d = \mathcal{P}_{\mathbf{L}_f}\boldsymbol{\lambda}$, are selected as the problem unknowns. It is well known [54] that this minimization problem is associated with the Lagrangian:

$$\mathscr{W}_\lambda\left(\boldsymbol{\lambda}_d, \boldsymbol{\mu}_b\right) = \tfrac{1}{2}\boldsymbol{\lambda}_d^{\mathsf{T}}\mathbf{F}_{bb}\boldsymbol{\lambda}_d - \mathbf{b}_\lambda^{\mathsf{T}}\boldsymbol{\lambda}_d + \boldsymbol{\mu}_b^{\mathsf{T}}\left(\mathbf{b}_\lambda - \mathbf{F}_{bb}\boldsymbol{\lambda}_d\right) \tag{55}$$

where a new variable $\boldsymbol{\mu}_b = \mathbf{C}_b\boldsymbol{\mu}$, representing a vector of Lagrange multipliers, is introduced to enforce the constraints. Furthermore, from the first-order optimality condition of this functional, the following system arises:

$$\begin{bmatrix} \mathcal{P}_{\mathbf{L}_f}^{\mathsf{T}}\mathbf{F}_{bb}\mathcal{P}_{\mathbf{L}_f} & \mathcal{P}_{\mathbf{L}_f}^{\mathsf{T}}\mathbf{F}_{bb}\mathbf{C}_b \\ \mathbf{C}_b^{\mathsf{T}}\mathbf{F}_{bb}\mathcal{P}_{\mathbf{L}_f}^{\mathsf{T}} & \mathbf{0} \end{bmatrix} \begin{Bmatrix} \boldsymbol{\lambda} \\ \boldsymbol{\mu} \end{Bmatrix}^{n+1} = \begin{Bmatrix} \mathbf{b}_\lambda \\ \mathbf{0} \end{Bmatrix}^{n+1} \tag{56}$$

a saddle-point problem equivalent to the initial quadratic minimization problem with constraints.

Remark 8. In AFETI methods, the classical PCG iterative solver described in Algorithm 1 needs to apply a projector $\mathcal{P}$ two times per iteration. When adopting complicated projectors, like in AFETI-1 with (43) or AFETI-2 with (47), the projection step becomes the most expensive operation creating a bottleneck in the algorithm performance. This effect can be alleviated by introducing simple modifications into the PCG algorithm. The basic idea here is to solve the AFETI-B system (14), with the simplest projector (17), enforcing the constraints directly on the search directions of the PCG solver during the iterative resolution process. This new algorithm is denominated AFETI-C.

6.1. Construction of the boundary constraints matrix

In the AFETI-C algorithm we group all the constraints, namely rigid-body and deformational modes, together into a single diagonal block matrix:

$$\mathbf{C}_i = [\mathbf{R}_i|\boldsymbol{\Phi}_i] \quad (i = 1 \cdots N) \quad \Rightarrow \quad \mathbf{C} = \begin{bmatrix} \mathbf{C}_1 & \cdots & \mathbf{0} \\ \vdots & \ddots & \vdots \\ \mathbf{0} & \cdots & \mathbf{C}_N \end{bmatrix} \tag{57}$$

where $\boldsymbol{\Phi}_i \in \mathbb{R}^{n_i \times n_d}$ corresponds to the lower deformational modes of the i^{th} partition and n_d is the number of these deformational modes included as constraints per subdomain. For computational efficiency, the lower modes are obtained for each substructure using inverse iteration based methods. Note that the computation of these modes suppose an extra computational effort, but their calculation is required only once. After that, the constraint matrix is computed as $\mathbf{C}_b = \mathbf{B}^{\mathsf{T}}\mathbf{C}$, a block diagonal matrix defining substructure-by-substructure the boundary linear constraints.

Remark 9. The construction of a matrix $\mathbf{C}$ combining the rigid-body modes plus corner equilibrium constraints and combined with a two-level decomposition was proposed by Farhat et al. [25, 26, 55] in the context of FETI for the solution of plate and shell problems.

6.2. The proposed AFETI-C algorithm

For the solution of the saddle point problem (56), we adopt AFETI-B with the residual $\mathbf{r}_\lambda(\boldsymbol{\lambda}) = \mathbf{0}$ defined in (18), subject to the extra constraint:

$$\mathbf{C}_b^\mathsf{T} \left(\mathbf{b}_\lambda - \mathbf{F}_{bb} \mathcal{P}_{\mathbf{L}_f} \boldsymbol{\lambda} \right) = \mathbf{0} \tag{58}$$

that will be enforced during the PCG iterative process. For this purpose, we propose the following structure for the solution:

$$\boldsymbol{\lambda} = \mathcal{P}_{\mathbf{L}_f} \left\{ \mathbf{C}_b \boldsymbol{\lambda}_{c0} + \sum_k \left(\boldsymbol{\lambda}_k + \mathbf{C}_b \boldsymbol{\lambda}_{ck} \right) \right\} \tag{59}$$

where subindex k indicates the iteration number, $\boldsymbol{\lambda}_k$ is the search direction obtained by the classical PCG Krylov subspace iteration and $\boldsymbol{\lambda}_{ck}$ is a correction of the k-th search direction introduced to fulfill the residual constraint (58).

The AFETI-C computes the initial component to identically satisfy the residual constraint and the rest of the search directions are modified so they do not contribute to the constrained residual. Then, the iterative process continues until the norm of the residual is smaller than a predefined tolerance.

The first term of the solution, $\boldsymbol{\lambda}_{c0}$, is obtained forcing the fulfillment of the residual constraint (58):

$$\mathbf{C}_b^\mathsf{T} \mathcal{P}_{\mathbf{L}_f}^\mathsf{T} \left\{ \mathbf{b}_\lambda - \mathbf{F}_{bb} \mathcal{P}_{\mathbf{L}_f} \mathbf{C}_b \boldsymbol{\lambda}_{c0} \right\} = \mathbf{0} \tag{60}$$

producing a coarse problem:

$$\left[\mathbf{C}_b^\mathsf{T} \boldsymbol{\Psi} \mathbf{C}_b \right] \boldsymbol{\lambda}_{c0} = \mathbf{C}_b^\mathsf{T} \mathcal{P}_{\mathbf{L}_f}^\mathsf{T} \mathbf{b}_\lambda \tag{61}$$

with a reduced dimension, equal to the total number of constraints imposed to the residual.

After the initial component has been computed, we proceed with the Krylov subspace iteration and for every new search direction $\boldsymbol{\lambda}_k$, that in general will not satisfy the constraint equation, we compute a modification $\boldsymbol{\lambda}_{ck}$ by imposing the constraint:

$$\mathbf{C}_b^\mathsf{T} \mathcal{P}_{\mathbf{L}_f}^\mathsf{T} \left\{ \mathbf{F}_{bb} \mathcal{P}_{\mathbf{L}_f} \left(\boldsymbol{\lambda}_k + \mathbf{C}_b \boldsymbol{\lambda}_{ck} \right) \right\} = \mathbf{0} \tag{62}$$

to eliminate the contribution of the new direction to the constrained residual. This modification vector

Algorithm 2 Preconditioned conjugate-gradient (PCG) with constraints. This algorithm solves for $\mathcal{P}\mathbf{x}$ by minimizing the residual $\mathbf{r}(\mathbf{x}) = \mathcal{P}^{\mathsf{T}}\{\mathbf{b} - \mathbf{A}\mathbf{x}\}$ using the preconditioner $\mathbf{A}^{+}$ and enforcing the constraint $\mathbf{C}^{\mathsf{T}}\mathbf{r} = \mathbf{0}$ to the search directions.

$\left[\mathbf{C}^{\mathsf{T}}\mathcal{P}^{\mathsf{T}}\mathbf{A}\mathcal{P}\mathbf{C}\right]\mathbf{e}_0 = \mathbf{C}^{\mathsf{T}}\mathcal{P}^{\mathsf{T}}\mathbf{b}$ ▷ Solve initial coarse problem

$\mathbf{x}_0 = \mathcal{P}\mathbf{C}\,\mathbf{e}_0$ ▷ Compute initial solution thus $\mathbf{C}^{\mathsf{T}}\mathcal{P}^{\mathsf{T}}(\mathbf{b} - \mathbf{A}\mathbf{x}_0) = \mathbf{0}$

$\mathbf{r}_0 = \mathcal{P}^{\mathsf{T}}\{\mathbf{b} - \mathbf{A}\mathbf{x}_0\}$ ▷ Initial projected residual

k=0 ▷ Initialize iteration counter

while $\|\mathbf{r}_{k+1}\|/\|\mathbf{r}_0\| > \varepsilon$ **do** ▷ Check convergence

  $\mathbf{z}_k = \mathbf{A}^{+}\mathbf{r}_k$ ▷ Precondition step

  $\left[\mathbf{C}^{\mathsf{T}}\mathcal{P}^{\mathsf{T}}\mathbf{A}\mathcal{P}\mathbf{C}\right]\mathbf{e}_k = -\mathbf{C}^{\mathsf{T}}\mathcal{P}^{\mathsf{T}}\mathbf{A}\mathcal{P}\mathbf{z}_k$ ▷ Solve coarse problem for correction $\mathbf{e}_k$

  $\mathbf{y}_k = \mathcal{P}(\mathbf{z}_k + \mathbf{C}\mathbf{e}_k)$ ▷ Correct direction to enforce $\mathbf{C}^{\mathsf{T}}\mathcal{P}^{\mathsf{T}}\mathbf{A}\mathbf{y}_k = \mathbf{0}$

  $\beta_k = \frac{\mathbf{y}_k^{\mathsf{T}}\mathbf{r}_k}{\mathbf{y}_{k-1}^{\mathsf{T}}\mathbf{r}_{k-1}}$ ▷ Conjugation (for $k = 0$, set $\beta_0 = 0$)

  $\mathbf{s}_k = \mathbf{y}_k + \beta_k\mathbf{s}_{k-1}$ ▷ Search direction (for $k = 0$, set $\mathbf{s}_0 = \mathbf{y}_0$)

  $\mathbf{d}_k = \mathbf{A}\mathbf{s}_k$ ▷ Solution step

  $\alpha_k = \frac{\mathbf{y}_k^{\mathsf{T}}\mathbf{r}_k}{\mathbf{s}_k^{\mathsf{T}}\mathbf{d}_k}$ ▷ Minimization

  $\mathbf{x}_{k+1} = \mathbf{x}_k + \alpha_k\mathbf{s}_k$ ▷ Update solution

  $\mathbf{r}_{k+1} = \mathbf{r}_k - \alpha_k\mathcal{P}^{\mathsf{T}}\mathbf{d}_k$ ▷ Update projected residual

  $k \leftarrow k + 1$ ▷ Increment iteration counter

end while ▷ Repeat until convergence

is calculated solving with iterative methods the coarse problem:

$$\left[\mathbf{C}_b^{\mathsf{T}}\mathbf{\Psi}\mathbf{C}_b\right]\boldsymbol{\lambda}_{ck} = -\mathbf{C}_b^{\mathsf{T}}\mathbf{\Psi}\boldsymbol{\lambda}_k \tag{63}$$

to obtain the modification of the direction $\boldsymbol{\lambda}_{ck}$ that is added to the search direction $\boldsymbol{\lambda}_k$ to complete the constrained solution component. Thanks to the simplicity of the projector $\mathcal{P}_{\mathbf{L}_f}$ and the localized character of the boundary flexibility $\mathbf{F}_{bb}$, this problem can be solved in a fully parallel manner requiring minimum interprocess communication.

The complete solution process of AFETI-C is summarized in Algorithm 2, that is reproduced substituting $\mathcal{P} = \mathcal{P}_{\mathbf{L}_f}$ as projector, the constraint matrix $\mathbf{C} = \mathbf{C}_b$ and the system matrix $\mathbf{A} = \mathbf{F}_{bb}$, together with the lumped preconditioner defined in (19). Note that, in order to enforce the global equilibrium at each iteration, the PCG Algorithm 1 has been enhanced with two simple steps. When we obtain a new candidate $\mathbf{z}_k$ for our solution vector, that in general will not satisfy the constraints, we calculate a correction of the solution component $\mathbf{e}_k$ and after that we compute the modified component $\mathbf{y}_k$, see Algorithm 2.

Remark 10. Using only the RBMs as constraints, i.e. constraint matrix $\mathbf{C}_b = \mathbf{R}_b$, we obtain an algorithm equivalent to AFETI-1 described in Section 4.1, with the advantage of substituting two

applications per iteration of a complicated projector $\mathcal{P}^{\mathbf{\Psi}}_{\mathbf{R}_b}$, needed by Algorithm 1, by the application of a simpler projector $\mathcal{P}_{\mathbf{L}_f}$ plus the solution of a coarse problem in Algorithm 2.

Remark 11. It was demonstrated in Section 5, that the residual constraint (58) using as constraints the rigid body modes, i.e., $\mathbf{C}_b = \mathbf{R}_b$, enforces global equilibrium in the substructures. In that particular case, the convergence properties of AFETI-1 are exactly the same than AFETI-C without deformational modes.

6.2.1. Regularization of the AFETI system

Considering that the localized method of Lagrange multipliers utilizes different Lagrange multipliers for each substructure, it is possible to introduce independent normalization factors for each group of Lagrange multipliers. This way the system is regularized, controlling the condition number of the final system [13, 14, 49].

In our case, the regularization process is done by performing in the basic AFETI system (12) the change of variable $\mathbf{u} = \mathbf{S}_u\hat{\mathbf{u}}$ and $\boldsymbol{\lambda} = \mathbf{S}_\lambda\hat{\boldsymbol{\lambda}}$, where $\mathbf{S}_u$ and $\mathbf{S}_\lambda$ are linear transformations, to obtain an equivalent system:

$$\begin{bmatrix} \mathbf{S}_u^\mathsf{T}\mathbf{K}_d\mathbf{S}_u & \mathbf{S}_u^\mathsf{T}\mathbf{B}\mathbf{S}_\lambda & \mathbf{0} \\ \mathbf{S}_\lambda^\mathsf{T}\mathbf{B}^\mathsf{T}\mathbf{S}_u & \mathbf{0} & -\mathbf{S}_\lambda^\mathsf{T}\mathbf{L}_f \\ \mathbf{0} & -\mathbf{L}_f^\mathsf{T}\mathbf{S}_\lambda & \mathbf{0} \end{bmatrix} \begin{Bmatrix} \hat{\ddot{\mathbf{u}}} \\ \hat{\boldsymbol{\lambda}} \\ \ddot{\mathbf{u}}_f \end{Bmatrix}^{n+1} = \begin{Bmatrix} \mathbf{S}_u^\mathsf{T}\mathbf{g}_u \\ \mathbf{0} \\ \mathbf{0} \end{Bmatrix}^{n+1} \tag{64}$$

that can be solved using the same AFETI solver. To regularize the system coefficients, our choice is to define $\mathbf{S}_u = \mathbf{diag}\left(\mathbf{K}_d\right)^{-\frac{1}{2}}$ and $\mathbf{S}_\lambda = \mathbf{diag}\left(\mathbf{B}^\mathsf{T}\mathbf{K}_d\mathbf{B}\right)^{\frac{1}{2}}$, so the new boundary extraction matrix $\mathbf{S}_u^\mathsf{T}\mathbf{B}\mathbf{S}_\lambda$ is of order one. For a subsequent application of the AFETI-C algorithm, the constraints matrix (57) should also be scaled using $\hat{\mathbf{C}} = \mathbf{S}_u^{-1}\mathbf{C}$ to produce a scaled boundary constraints matrix $\hat{\mathbf{C}}_b = \mathbf{S}_\lambda^\mathsf{T}\mathbf{B}^\mathsf{T}\mathbf{C}$. Although this regularization process is not necessary for second order problems with displacement DOFs, we will demonstrate in Section 7 that its use becomes imperative for plate and shell finite elements.

7. Numerical examples

In this section, the performance of the proposed AFETI methods is assessed for second order and fourth order linear elastic problems. For this task, we will solve different example problems using the AFETI-1 method described in Section 4.1 and the proposed AFETI-C equipped with different number n_d of deformational modes, as described in Section 6.2. It will be particularly interesting to study the effect of introducing different number of deformational constraints in the convergence of the AFETI-C algorithm developed in the paper.

In all the examples, time integration is performed using the Newmark method with parameters $\beta = \frac{1}{4}$ and $\gamma = \frac{1}{2}$ to ensure unconditional stability. For all cases, the same convergence criterion is used, based on the relative error of the residual:

$$\frac{\|\mathbf{r}_{k+1}\|_2}{\|\mathbf{r}_0\|_2} < \varepsilon = 10^{-4} \tag{65}$$

where $\mathbf{r}_{k+1}$ is the projected residual at iteration $(k+1)$, see Algorithms 1 and 2. The convergence results presented, correspond to the first time-step solution, obtained using the corresponding dynamic algorithm equipped with the simple lumped preconditioner given by (19).

7.1. Second-order elasticity problems

We start the study with second order elasticity problems discretized with pure displacement finite elements. In this case and assuming material homogeneity, the AFETI system is well behaved and the regularization process described in Section 6.2.1 is not used.

7.1.1. Plane elasticity in a unit square

The first problem considered is a homogeneous and elastic two-dimensional plate modeled with four node quadrilateral elements. The mesh is defined in a square domain $\Omega = [0,1] \times [0,1]$ that is partitioned into N regular subdomains of size H and element size h, see Figure 3. The nodes located on the two left corners of the domain are completely fixed and it is considered the effect of a sudden vertical uniform body load of value $g = 9.81$. This body load is applied entirely at the first time step of the simulation producing a transient response that is integrated in time with a fixed time step $\Delta t = 0.025$.

Figure 3 (right) demonstrates the influence of RBM equilibrium enforcement during iterations in the convergence of different AFETI methods. For a particular case of $N = 5 \times 5$ partitions with 10×10 elements per partition, it is compared the convergence of the basic AFETI-B algorithm, with AFETI-1 and AFETI-C, without using deformational-mode constraints, i.e. $n_d = 0$. It is observed that AFETI-C, equipped with the RBMs as constraints, is completely equivalent to AFETI-1. As previously mentioned, for second order elastic problems and introducing the RBMs as constraints, produces fast convergence to the solution. Now, the question arises if it is possible to improve that convergence rate by including deformational modes as extra constraints.

The answer to this question is contained in Figure 4. Now, maintaining the same element size h, the number of subdomains N is varied to study also the influence of partitioning in the global convergence of AFETI-C. Specifically, two different values of $N = \{9, 36\}$, respectively with $H/h = \{20, 10\}$, are considered. First observation is that for $n_d = 0$, including only RBMs as constraints, we need approximately three iterations to reduce the residual one order of magnitude and the total number

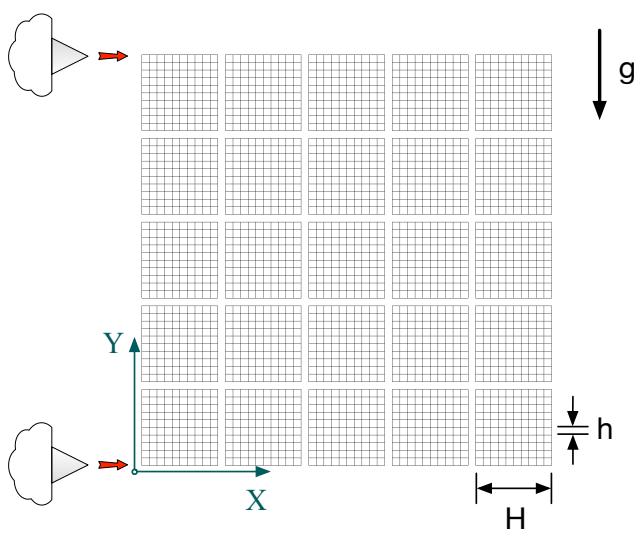

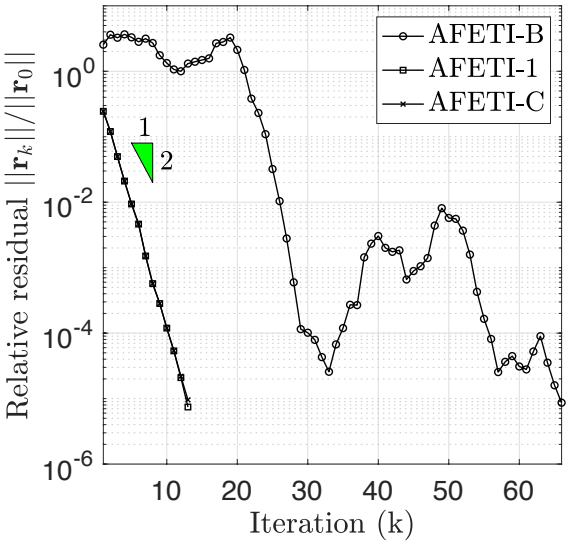

Figure 3: Regularly partitioned mesh with $N = 5 \times 5$ subdomains of side dimension $H = 1/5$, where each subdomain is composed of 10×10 quadrilateral elements of size $h = H/10$ (left). Convergence of the AFETI-B method without global equilibrium enforcement, the one-level AFETI-1 and the constrained AFETI-C with $n_d = 0$, obtained for the particular case $N = 5 \times 5$ and $h = H/20$ (right). The triangle with slope $1/2$ indicates a reduction of the residual by a factor of two per iteration.

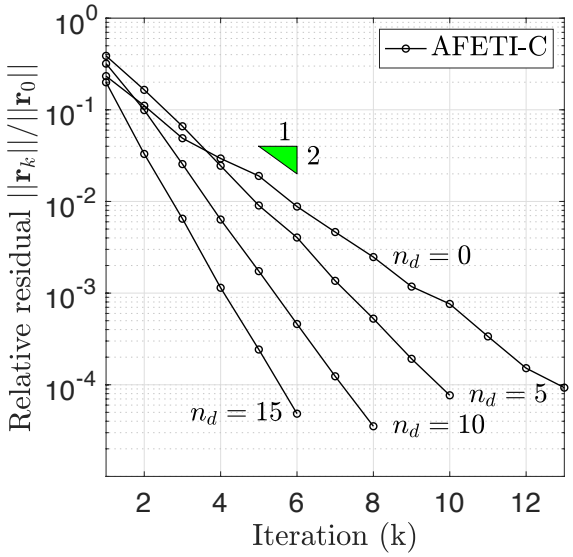

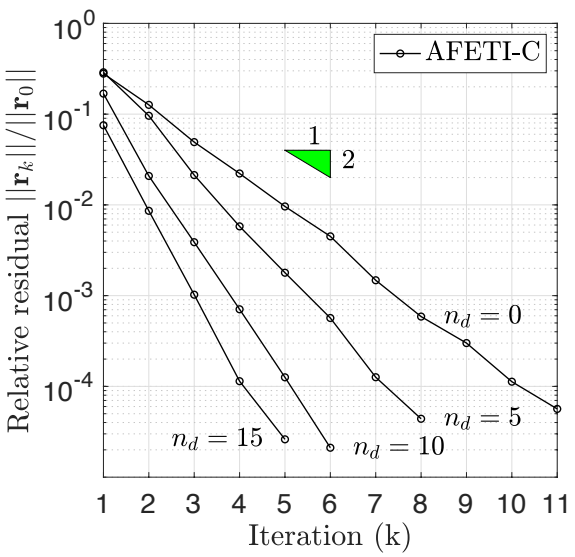

Figure 4: Convergence of the regular 2D plate problem for $N = 3 \times 3$ subdomains of 20×20 elements (left) and $N = 6 \times 6$ subdomains of 10×10 elements (right) using AFETI-C equipped with different number of deformational-mode residual constrains $n_d = \{0, 5, 10, 15\}$. Higher convergence rates are observed when deformational modes are included as additional constraints.

Partitions	H/h	AFETI-C (ms)			
		$n_d = 0$	$n_d = 5$	$n_d = 10$	$n_d = 15$
$N = 3 \times 3$	20	28.6	21.4	16.7	17.1
$N = 6 \times 6$	10	37.7	34.7	43.1	57.3

Table 1: Execution times of the elastic unit square problem. Wall clock time (in milliseconds) required by AFETI-C to solve the cases contained in Figure 4.

of iterations is not severely affected by the partitioning. This result is a well known scalability property of FETI-T for elastic problems. The same problem has been studied with two-level FETI including rigid body motions in the projector [45]. In particular, for $H/h = 40$, FETI-T equipped with the lumped preconditioner requires between $17 - 30$ iterations for a convergence criterion of 10^{-6} on the global primal residual, that is in agreement with our experience.

We introduce $n_d = \{0, 5, 10, 15\}$ extra deformational modes in AFETI-C as constraints, increasing at the same time the size of the coarse problem to $N \cdot (n_\alpha + n_d)$, where $n_\alpha = 3$ is the number of RBMs per substructure. A rapid acceleration of the convergence is clearly observed in Figure 4, with a progressive increase in the order of convergence with the number of deformational modes included. A reasonable number of deformational modes to use per subdomain is $n_d = 5$, solving the problem in $8 - 10$ iterations. Moreover, by introducing $n_d = 15$ deformational constraints per subdomain, it is possible to reduce the residual one order of magnitude in less than two iterations.

Finally, it is reported in Table 1 the wall clock time required by AFETI-C running Algorithm 2 to solve the cases contained in Figure 4. Analyzing the execution times we observe that, for a fixed number of partitions, there exists an optimum number of deformational modes that minimizes the execution time. In our case, $n_d = 10$ for $H/h = 20$ and $n_d = 5$ for $H/h = 10$. It is also observed that this optimum number of deformational modes, to be included as residual constraints, increases with the number of elements per partition, i.e., with the size of the interface problem.

7.1.2. Concrete gravity dam

Next, we move to a more realistic three dimensional example with a relatively complex geometry. It is the case of a concrete gravity dam with seven spillways, represented in Figure 5, with dimensions: 67 m high, 50 m wide and 210 m long. The elastic material properties of the structure correspond to plain concrete, with elastic modulus $E_c = 20\,\text{GPa}$, Poisson's ratio $\nu_c = 0.2$ and density $\rho_c = 2450\,\text{kg/m}^3$. The geometry is discretized using 45,496 tetrahedral elements and 10,589 nodes, with a total of 31,767 displacement DOFs. All the nodes located at the bottom plane of the dam are fixed in the three directions, and a uniform body load due to vertical gravity acceleration is applied to all elements at the

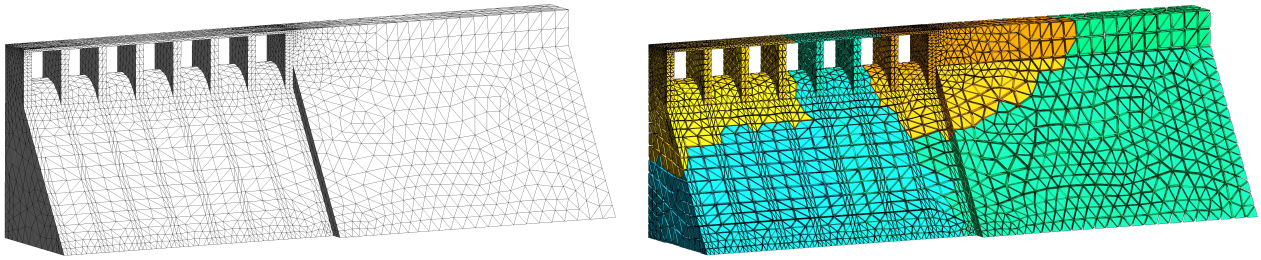

Figure 5: Finite element model of a gravity dam with seven spillways. The mesh is composed of 45,496 tetrahedral elements and 10,589 nodes (left) and partitioned into $N = 5$ substructures using the recursive algorithm of METIS (right).

		AFETI-C				
Partitions	**AFETI-1**	$n_d = 4$	$n_d = 8$	$n_d = 12$	$n_d = 16$	$n_d = 20$
$N = 6$	31	26	23	19	18	17
$N = 8$	35	27	24	23	21	20
$N = 10$	36	28	23	20	19	18
$N = 12$	39	31	23	21	19	18

Table 2: Iterations of the PCG algorithm for the 3D dam problem with AFETI-1 and AFETI-C equipped with $n_d = \{4, 8, 12, 14, 20\}$ deformational-mode residual constraints. Note that for $n_d = 0$, AFETI-C needs the same number of iterations than AFETI-1.

initial instant of the simulation. Time integration step size is fixed to $\Delta t = 0.025$ s.

The problem is first solved with algorithm AFETI-1. For this purpose, the finite element mesh is partitioned into $N = \{6, 8, 10, 12\}$ substructures using the recursive algorithm of METIS [56] and the first time step solved by reducing the residual (45) with the classical PCG, described in Algorithm 1. The results are presented in the second column of Table 2, where it is observed that increasing the number of partitions produces a small influence in the total number of iterations required for convergence. Although the effect is more pronounced than that observed in the previous example with regular partitions. Note that here we are dealing with highly irregular partitions.

Then, we solve exactly the same problem with AFETI-C introducing a different number $n_d = \{4, 8, 12, 14, 20\}$ of deformational-mode residual constraints. The results contained in Table 2 demonstrate the scalability of the AFETI-C method, where the total number of iterations performed now by Algorithm 2 is mildly affected by the number of partitions N used to divide the mesh. It is also observed that the optimal number of deformational modes to utilize is $n_d \sim 8 - 10$, that produces a reduction in the number of iterations between 30% and 50% without overloading the size of the coarse problem. This conclusion is also in accordance with the behavior of AFETI-C observed in two-dimensional problems.

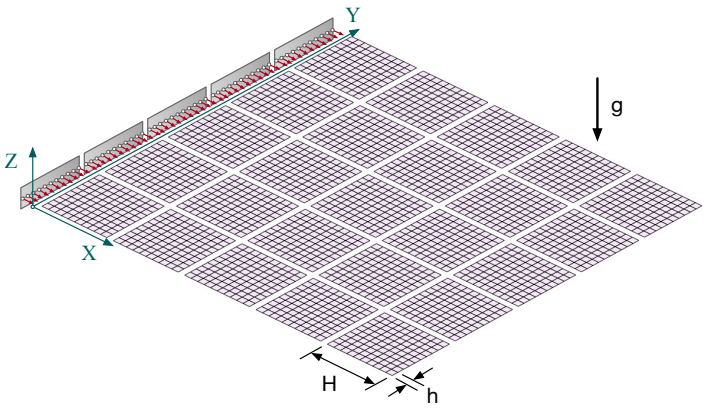

Figure 6: Model of a cantilever plate fixed at $X = 0$ composed of 2,500 quadrilateral 4-node ANS C^0 plate elements with 2,601 nodes and 7,803 DOFs. The mesh is partitioned into $N = 5 \times 5$ identical substructures of size $H = 1/5$ and 10×10 elements of size $h = H/10$.

7.2. Fourth-order elasticity problems

The inherent difficulties associated to the solution of fourth-order elasticity problems with FETI methods are well described in the literature [22, 25, 26, 47]. The main problem lies in the ill-conditioning of the system matrices, due to the combination of displacement and rotation DOFs present in plate and shell structural elements.

7.2.1. Plate bending

First we consider a simple and regular geometry, studying the case of a square cantilevered plate of side length $L = 1$ and thickness $t = 0.01$. The selected material properties are $E = 1 \times 10^6$, Poisson's ratio $\nu = 0.3$ and density $\rho = 1000$. Again, a constant gravity body load $g = 9.81$ is applied entirely at the first time step of the simulation, but now the time integration step is fixed to $\Delta t = 0.05 \approx \frac{T_1}{150}$, where T_1 is the first period of the structure. The plate is discretized with a regular mesh of 50×50 quadrilateral 4-ANS C^0 plate elements of three DOFs per node, vertical displacement ant the two plane rotations. Then, the mesh is partitioned into $N = 5 \times 5$ identical substructures of size $H = 1/5$ and 10×10 elements per subdomain of size $h = H/10$, see Figure 6.

Using AFETI-C, the problem is solved with and without regularization, obtaining the results shown in Figure 7. For both cases, the effect of including deformational interface residual constraints is studied varying $n_d = \{0, 5, 10, 15\}$. We observe that without deformational modes, $n_d = 0$, convergence is uniform but very slow (left) and regularization (right) has a small influence, reducing the required number of iterations from 73 to 69.

Without regularization, the total number of iterations is divided by two after augmenting the number of deformational constraints to $n_d = 15$, at the cost of increasing the size of the coarse problem. However,

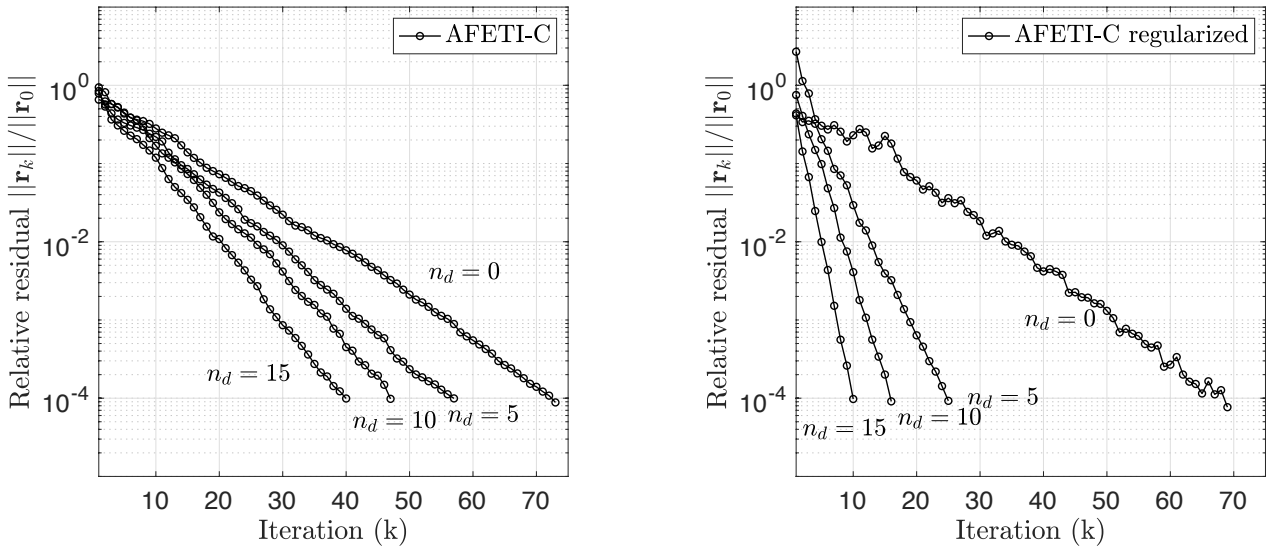

Figure 7: Effect of regularization in the convergence of the 3D plate problem with $N = 5 \times 5$ subdomains of 10×10 elements and different number of deformational-mode residual constrains $n_d = \{0, 5, 10, 15\}$. Convergence of AFETI-C without system regularization (left) and AFETI-C with system regularization (right).

combining deformational modes with regularization has a tremendous impact on the convergence, where the required number of iterations is now reduced by a factor of 7 after introducing $n_d = 15$ deformation constraints in the residual. The same plate bending problem was studied in [25] using a two-level decomposition method specifically designed for plates and shells, requiring around 30 iterations when PCG is equipped with the lumped preconditioner. In our case, this level of convergence can be achieved with AFETI-C using $n_d = 5$ deformational modes with system regularization.

7.2.2. Semi-cylindrical shell

This final example is taken from Fragakis et al. [57] and considers a semi-cylindrical panel under the action of uniform gravity load, see Figure 8. The radius of the panel is $R = 0.5$, its length $L = 1.6$ and the thickness $t = 0.01$. We assume pure elastic behavior, with Young's modulus $E = 1 \times 10^6$, Poisson ratio $\nu = 0.30$ and material density $\rho = 1000$. The panel is modeled with triangular ANS shell elements [58] of 6 DOFs per node, using a structured mesh of 131×131 nodes. Furthermore, the nodes located at $Z = 0$ are completely fixed along the two linear edges of the panel. The model has 102,966 DOFs and is decomposed into 130 irregular subdomains using the partitioning library METIS, as depicted in Figure 8 (right). The time step for time integration is set to $\Delta t = 0.05 \approx \frac{T_1}{120}$, with T_1 the first period of the structure.

In Figure 9, convergence results with (left) and without (right) regularization are presented for different number of deformational modes. It is observed a similar behavior than in the previous example, the benefit of using regularization without deformational interface constraints ($n_d = 0$) is very

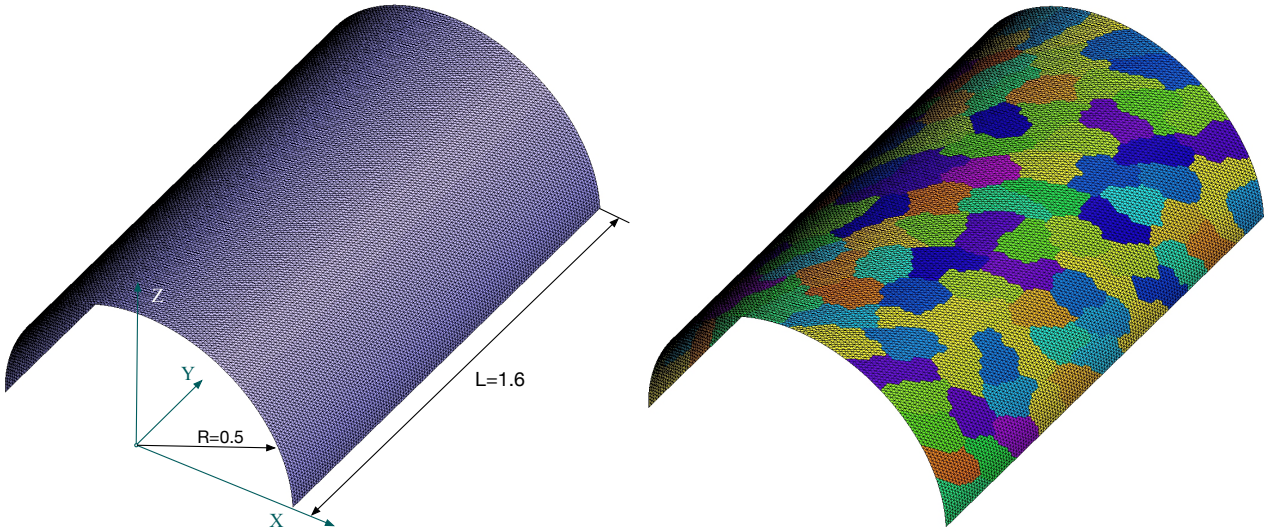

Figure 8: Dimensions and finite element model of a semi-cylindrical shell with 33,800 triangular ANS shell elements and 17,161 nodes with 6 DOFs per node (left). Same mesh partitioned into $N = 130$ substructures using the recursive algorithm of METIS (right).

modest, reducing from 180 to 144 the required number of iterations. Without regularization, between $130 - 180$ iterations are needed for convergence depending on the number of deformational constraints $n_d = \{0, 5, 10, 15\}$ used in the coarse problem. Using regularization and $n_d = 15$ deformational modes, the required number of iterations is divided by 7 and reduced to a total of 19 iterations for convergence. The same problem, modeled with triangular TRIC shell elements and solved with classical FETI methods using coarse problem embedded in the preconditioner [57], required 202 iterations for FETI-T, 75 iterations for FETI-T equipped with special precondition, while FETI-DP only needed 39 iterations. This means that FETI-DP is able to divide by a factor of 5 the total number of iterations required by FETI-T and approximately reduces the residual by about one order of magnitude every 10 iterations.

For this particular experiment, we find that AFETI-C with regularization and 5 deformational modes is able to perform similar performance than FETI-DP. More importantly, the number of iterations can be progressively reduced by introducing more deformational constraints.

8. Conclusions

A variational framework for a formal derivation of partitioned analysis methods with localized Lagrange multipliers is proposed. A distinct feature of the present variational formulation is an *a priori* inclusion of the rigid-body motions of the substructures. We summarize our findings in the following:

- One-level AFETI-1, with coarse problem included in the projector, can be considered the AFETI alternative to FETI-T with equivalent properties. It enforces RBM equilibrium of the substructures

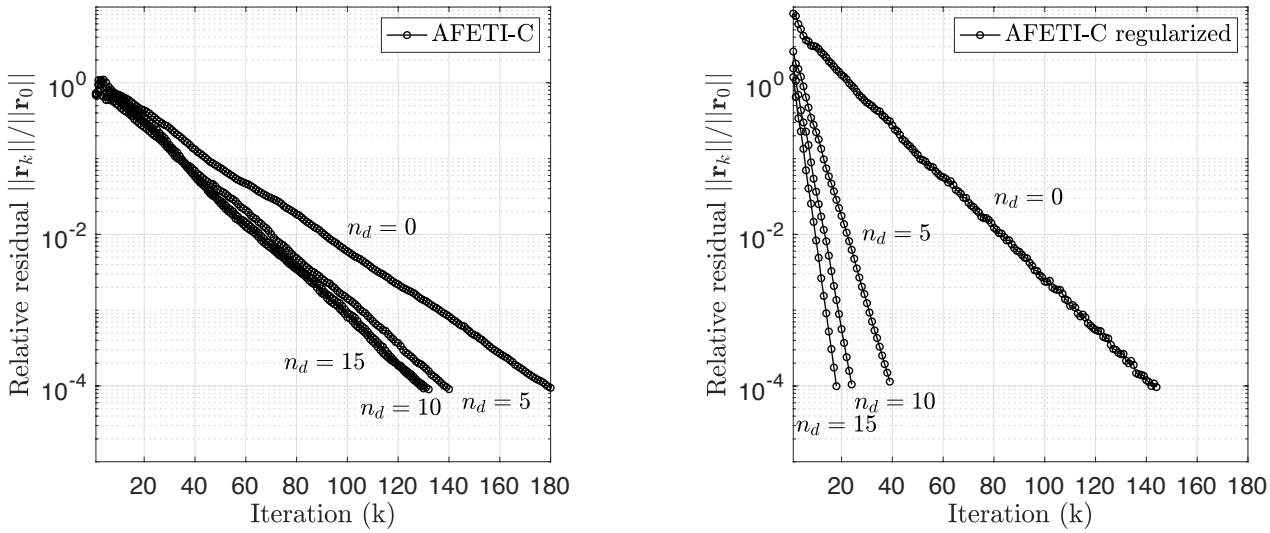

Figure 9: Convergence results of the semi-cylindrical shell problem with AFETI-C and different number $n_d = \{0, 5, 10, 15\}$ of deformational modes, without system regularization (left) and including regularization of the system (right). Regularization for $n_d = 0$ produces a modest gain in the convergence of 36 iterations, but provides a dramatic improvement when deformational modes are included as additional interface constraints.

and requires application of the projector twice per PCG iteration.

- Two-level AFETI-2 embodies a complicated projector that enforces RBM equilibrium and extra constraints in two different steps. However, its implementation is considered excessively complicated and extremely expensive for numerical applications.

- One-level AFETI-C is considered the simplest alternative, requiring the solution of only one coarse problem solution per iteration. Interface constraints come from rigid and deformational modes that can be computed locally in the partitions and reused for every time step.

- AFETI-C with heterogeneity regularization and infusion of a small number of interface deformational modes is considered the best candidate for fourth order problems, providing iteration counts that are competitive with existing parallel solution algorithms and implementation simplicity.

In comparing the proposed AFETI-C method with the FETI-DP method, it is noted that in FETI-DP the elimination of global corner nodes from the system, produces a final symmetric and positive definite linear system with an embedded coarse problem that is solved by PCG iteration, just like the original FETI method. Hence, one difficulty of the method lies in the evaluation of the coarse problem operator that are functions of the interface flexibilities and the inverse of the Schur complement of the dynamic stiffness associated to the corner nodes. This Schur complement matrix involves a global assembly that requires interprocess communications for its construction. In contrast, the AFETI-C coarse problem (61) is a completely partitioned system, where the rigid and deformational constraints of

partitioned domains can be computed and applied locally for each partition with minimum interprocess communication.

In conclusion, the proposed AFETI-C algorithm is easy to understand, simple to implement and employs the same solution strategy developed for static problems. It turns out that regularization for handling system heterogeneities is easy to incorporate into the proposed AFETI-C and, unlike FETI-DP, it needs no special treatment of corners and cross points.

Appendix A. Review of null space methods and projectors

The projection operation is a basic ingredient of the FETI and AFETI methods. It is widely used in the derivation of many different FETI solution algorithms and much effort has been dedicated to describe and formalize its use, see for example the works by Farhat et al. [27] and Fragakis et al. [59, 57], defining its properties and operational algebra in a general FETI framework. In this Appendix we define the projection concept and summarize its basic properties under the AFETI framework. These properties are repeatedly used through the paper.

Appendix A.1. Introduction

The solution by projections of FETI saddle point problems, is known in mathematics as *null space methods* [54]. The null space approach has been extensively used in structural mechanics since the early 70s, initially known under the name of *force method* [60], where a vector $\boldsymbol{\lambda}$ of internal forces with constraints, that needs to satisfy the saddle point problem:

$$\begin{bmatrix} \mathbf{F} & \mathbf{B} \\ \mathbf{B}^{\mathsf{T}} & \mathbf{0} \end{bmatrix} \begin{Bmatrix} \boldsymbol{\lambda} \\ \mathbf{d} \end{Bmatrix} = \begin{Bmatrix} \mathbf{f} \\ \mathbf{g} \end{Bmatrix} \tag{A.1}$$

can be computed introducing the decomposition:

$$\boldsymbol{\lambda} = \mathcal{P}_{\mathbf{B}} \boldsymbol{\alpha} + \mathbf{B} \left[\mathbf{B}^{\mathsf{T}} \mathbf{B} \right]^{-1} \mathbf{g} \tag{A.2}$$

where $\mathcal{P}_{\mathbf{B}}$ is a linear operator that projects the new solution $\boldsymbol{\alpha}$ into the subspace orthogonal to the constraints matrix $\mathbf{B}$. This decomposition transforms the initial constrained problem (A.1) into the linear system:

$$\left[\mathcal{P}_{\mathbf{B}}{}^{\mathsf{T}} \mathbf{F} \mathcal{P}_{\mathbf{B}} \right] \boldsymbol{\alpha} = \mathbf{b} \tag{A.3}$$

with $\mathbf{b} = \mathcal{P}_{\mathbf{B}}{}^{\mathsf{T}} \left(\mathbf{f} - \mathbf{F}\mathbf{B} \left[\mathbf{B}^{\mathsf{T}} \mathbf{B} \right]^{-1} \mathbf{g} \right)$ and where the constraints are now enforced implicitly by the projector.

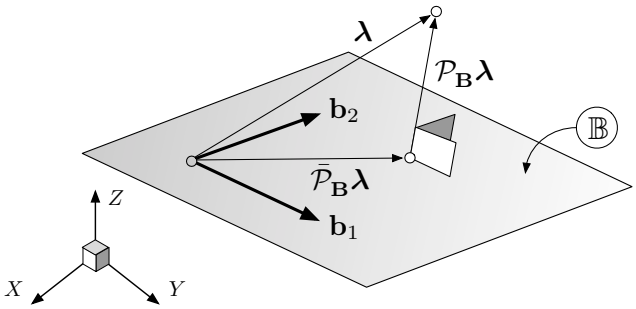

Figure A.10: Geometric representation in $\mathbb{R}^3$ of the projection operation into a subspace $\mathbb{B}$ with basis $\{\mathbf{b}_1, \mathbf{b}_2\}$. The projector $\bar{\mathcal{P}}_{\mathbf{B}}$ projects a vector $\boldsymbol{\lambda} \in \mathbb{R}^3$ into $\mathbb{B}$ while $\mathcal{P}_{\mathbf{B}}$ projects $\boldsymbol{\lambda}$ into $\mathbb{B}^{\perp}$, fulfilling the condition $\mathbf{B}^{\mathsf{T}}\mathcal{P}_{\mathbf{B}}\boldsymbol{\lambda} = \mathbf{0}$.

Appendix A.2. The projection operation

Definition 1. Let $\mathbb{B} \subset \mathbb{R}^n$ be a subspace with basis $\{\mathbf{b}_1, ..., \mathbf{b}_m\}$ and let $\mathbf{B} = [\mathbf{b}_1 ... \mathbf{b}_m] \in \mathbb{R}^{n \times m}$ be the matrix with columns $\mathbf{b}_i$. The symmetric projector $\bar{\mathcal{P}}_{\mathbf{B}} : \mathbb{R}^n \to \mathbb{B}$ given by

$$\bar{\mathcal{P}}_{\mathbf{B}} = \mathbf{B}\left[\mathbf{B}^{\mathsf{T}}\mathbf{B}\right]^{-1}\mathbf{B}^{\mathsf{T}} \tag{A.4}$$

is a linear and continuous mapping that projects every vector $\boldsymbol{\lambda} \in \mathbb{R}^n$ onto $\mathbb{B}$. As any projector, $\bar{\mathcal{P}}_{\mathbf{B}}$ is an idempotent operator, i.e., $\bar{\mathcal{P}}_{\mathbf{B}}\bar{\mathcal{P}}_{\mathbf{B}} = \bar{\mathcal{P}}_{\mathbf{B}}$.

Definition 2. Let $\mathbb{B}^{\perp} = \left\{\boldsymbol{\lambda} \in \mathbb{R}^n : \mathbf{B}^{\mathsf{T}}\boldsymbol{\lambda} = \mathbf{0}\right\}$ be the subspace of $\mathbb{R}^n$ orthogonal to $\mathbb{B}$ that extends its range to $\mathbb{R}^n = \mathbb{B} \oplus \mathbb{B}^{\perp}$. If $\mathbf{I} \in \mathbb{R}^{n \times n}$ is the identity matrix, then $\mathcal{P}_{\mathbf{B}} = \mathbf{I} - \bar{\mathcal{P}}_{\mathbf{B}}$ is also a projector that maps every $\boldsymbol{\lambda} \in \mathbb{R}^n$ onto $\mathbb{B}^{\perp}$. This property follows immediately from the identity $\boldsymbol{\lambda} = \bar{\mathcal{P}}_{\mathbf{B}}\boldsymbol{\lambda} + \left\{\boldsymbol{\lambda} - \bar{\mathcal{P}}_{\mathbf{B}}\boldsymbol{\lambda}\right\}$, (see Figure A.10). Finally, expressing $\boldsymbol{\lambda} \in \mathbb{R}^n$ as $\boldsymbol{\lambda} = \mathbf{A}\boldsymbol{\alpha} + \mathbf{B}\boldsymbol{\beta}$ using a matrix $\mathbf{A} \in \mathbb{R}^{n \times n}$ such that $\mathbf{B}^{\mathsf{T}}\mathbf{A} = \mathbf{0}$ with vectors $\boldsymbol{\alpha} \in \mathbb{R}^n$ and $\boldsymbol{\beta} \in \mathbb{R}^m$, we say that the projector $\mathcal{P}_{\mathbf{B}} : \mathbb{R}^n \to \mathbb{B}^{\perp}$ filters out (or eliminates) the components of $\boldsymbol{\lambda}$ in $\mathcal{R}(\mathbf{B})$ because $\mathcal{P}_{\mathbf{B}}\boldsymbol{\lambda} = \mathbf{A}\boldsymbol{\alpha}$.

Corollary 1. *Any vector $\boldsymbol{\lambda} \in \mathbb{R}^n$ can be decomposed with full support of $\mathbb{R}^n$ as*

$$\boldsymbol{\lambda} = \mathcal{P}_{\mathbf{B}}\boldsymbol{\alpha} + \mathbf{B}\boldsymbol{\beta} \tag{A.5}$$

by projection into orthogonal subspaces $\mathbb{B}^{\perp}$ and $\mathbb{B}$.

Appendix B. Projectors for FETI methods

Some particularities and extensions of the projection operation defined above have been used in the context of FETI methods. We summarize them as follows.

Definition 3. Let $\mathbf{A} \in \mathbb{R}^{n\times n}$ be an arbitrary symmetric matrix such that $\mathbf{B}^{\mathsf{T}}\mathbf{A}\mathbf{B} \in \mathbb{R}^{m\times m}$ is a positive definite matrix, we define a new $\mathbf{A}$-orthogonal projector $\mathcal{P}_{\mathbf{B}}^{\mathbf{A}}$ as

$$\mathcal{P}_{\mathbf{B}}^{\mathbf{A}} = \mathbf{I} - \mathbf{A}\mathbf{B}\left[\mathbf{B}^{\mathsf{T}}\mathbf{A}\mathbf{B}\right]^{-1}\mathbf{B}^{\mathsf{T}} \tag{B.1}$$

an idempotent and non-symmetric operator that eliminates the components of any vector $\boldsymbol{\lambda} \in \mathbb{R}^n$ in $\mathcal{R}(\mathbf{A}\mathbf{B})$. This filtering process is achieved thanks to the property

$$\mathcal{P}_{\mathbf{B}}^{\mathbf{A}}\mathbf{A}\mathbf{B} = \mathbf{0} \tag{B.2}$$

revealing that $\mathbf{A}\mathbf{B}$ belongs to the kernel of $\mathcal{P}_{\mathbf{B}}^{\mathbf{A}}$. Note also that the non symmetrical projector $\mathcal{P}_{\mathbf{B}}^{\mathbf{A}}$ presents the following symmetry

$$\mathcal{P}_{\mathbf{B}}^{\mathbf{A}}\mathbf{A} = \mathbf{A}\mathcal{P}_{\mathbf{B}}^{\mathbf{A}^{\mathsf{T}}} \tag{B.3}$$

with respect to matrix $\mathbf{A}$.

Proposition 1. *From definition (B.1) it follows that $\mathcal{P}_{\mathbf{B}}^{\mathbf{A}^{\mathsf{T}}} : \mathbb{R}^n \to \mathbb{B}^{\perp}$ is also a projector, thanks to property*

$$\mathcal{P}_{\mathbf{B}}^{\mathbf{A}^{\mathsf{T}}}\mathbf{B} = \mathbf{0} \tag{B.4}$$

meaning that $\mathcal{P}_{\mathbf{B}}^{\mathbf{A}^{\mathsf{T}}}$ applied to a general vector of $\mathbb{R}^n$ acts as a filter eliminating the components in $\mathcal{R}(\mathbf{B})$, i.e. projecting into $\mathbb{B}^{\perp}$.

Corollary 2. *Using projector (B.1) every vector $\boldsymbol{\lambda} \in \mathbb{R}^n$ can be decomposed with full support of $\mathbb{R}^n$, obtaining the one-level decompositions*

$$\boldsymbol{\lambda} = \mathcal{P}_{\mathbf{B}}^{\mathbf{A}}\boldsymbol{\alpha} + \mathbf{A}\mathbf{B}\boldsymbol{\beta} \tag{B.5}$$

$$\boldsymbol{\lambda} = \mathcal{P}_{\mathbf{B}}^{\mathbf{A}^{\mathsf{T}}}\boldsymbol{\alpha} + \mathbf{B}\boldsymbol{\beta} \tag{B.6}$$

based on properties (B.2) and (B.4). Moreover, a second decomposition of the vector $\boldsymbol{\alpha}$ can be introduced using (B.6) in (B.5) and vice-versa, obtaining the two-level decompositions

$$\boldsymbol{\lambda} = \mathcal{P}_{\mathbf{B}}^{\mathbf{A}}\left\{\mathcal{P}_{\mathbf{C}}^{\mathbf{D}^{\mathsf{T}}}\boldsymbol{\alpha} + \mathbf{C}\boldsymbol{\gamma}\right\} + \mathbf{A}\mathbf{B}\boldsymbol{\beta} \tag{B.7}$$

$$\boldsymbol{\lambda} = \mathcal{P}_{\mathbf{C}}^{\mathbf{D}^{\mathsf{T}}}\left\{\mathcal{P}_{\mathbf{B}}^{\mathbf{A}}\boldsymbol{\alpha} + \mathbf{A}\mathbf{B}\boldsymbol{\beta}\right\} + \mathbf{C}\boldsymbol{\gamma} \tag{B.8}$$

with $\mathbf{C} \in \mathbb{R}^{n\times p}$ and $\boldsymbol{\gamma} \in \mathbb{R}^p$, that are also valid decompositions of $\boldsymbol{\lambda}$.

Example 1. Given a constant vector $\mathbf{g} \in \mathbb{R}^m$, the space of all $\boldsymbol{\lambda} \in \mathbb{R}^n$ such that $\mathbf{B}^\mathsf{T}\boldsymbol{\lambda} = \mathbf{g}$ can be represented using the one-level decomposition (B.5) as

$$\boldsymbol{\lambda} = \mathcal{P}_{\mathbf{B}}^{\mathbf{A}}\boldsymbol{\alpha} + \mathbf{AB}\left[\mathbf{B}^\mathsf{T}\mathbf{AB}\right]^{-1}\mathbf{g} \tag{B.9}$$

with $\boldsymbol{\alpha} \in \mathbb{R}^n$.

Appendix C. Projectors for AFETI methods

An additional refinement within the projection concept is used for the derivation of AFETI algorithms.

Definition 4. The projector $\mathcal{P}_{\mathbf{R}}^{\boldsymbol{\Psi}^\mathsf{T}}$ where $\boldsymbol{\Psi} = \mathcal{P}_{\mathbf{B}}^{\mathbf{A}}\mathbf{F}\mathcal{P}_{\mathbf{B}}^{\mathbf{A}^\mathsf{T}}$, with matrices $\mathbf{F} \in \mathbb{R}^{n\times n}$ and $\mathbf{R} \in \mathbb{R}^{n\times q}$ such that $\mathbf{R}^\mathsf{T}\boldsymbol{\Psi}\mathbf{R} \in \mathbb{R}^{q\times q}$ is nonsingular, presents the following properties

$$\mathcal{P}_{\mathbf{R}}^{\boldsymbol{\Psi}^\mathsf{T}}\mathbf{R} = \mathbf{0} \tag{C.1}$$

$$\mathcal{P}_{\mathbf{R}}^{\boldsymbol{\Psi}^\mathsf{T}}\mathbf{B} = \mathbf{B} \tag{C.2}$$

i.e., acts as a filter of $\mathbf{R}$ components while retaining $\mathbf{B}$ components of a vector of $\mathbb{R}^n$.

Proposition 2. *Consequence of previous definition is that the composition* $\mathcal{P}_{\mathbf{B}}^{\mathbf{A}^\mathsf{T}}\mathcal{P}_{\mathbf{R}}^{\boldsymbol{\Psi}^\mathsf{T}}$ *is a double-filter of two different subspaces, that is,*

$$\mathcal{P}_{\mathbf{B}}^{\mathbf{A}^\mathsf{T}}\mathcal{P}_{\mathbf{R}}^{\boldsymbol{\Psi}^\mathsf{T}}\mathbf{R} = \mathbf{0} \tag{C.3}$$

$$\mathcal{P}_{\mathbf{B}}^{\mathbf{A}^\mathsf{T}}\mathcal{P}_{\mathbf{R}}^{\boldsymbol{\Psi}^\mathsf{T}}\mathbf{B} = \mathbf{0} \tag{C.4}$$

showing that it can be used to eliminate components of subspaces with basis $\mathbf{R}$ *and* $\mathbf{B}$*, with the additional property,*

$$\mathbf{R}^\mathsf{T}\mathcal{P}_{\mathbf{B}}^{\mathbf{A}}\mathbf{F}\mathcal{P}_{\mathbf{B}}^{\mathbf{A}^\mathsf{T}}\mathcal{P}_{\mathbf{R}}^{\boldsymbol{\Psi}^\mathsf{T}} = \mathbf{0} \tag{C.5}$$

Proof. Note that (C.3) is a direct consequence of (B.4), that (C.4) comes from the consecutive application of (C.2) and (B.4), and that (C.5) is property (B.2) transposed. □

Proposition 3. *The following symmetry condition holds between* $\mathcal{P}_{\mathbf{R}}^{\boldsymbol{\Psi}}$ *and* $\mathcal{P}_{\mathbf{B}}^{\mathbf{A}}$*:*

$$\mathcal{P}_{\mathbf{B}}^{\mathbf{A}}\mathcal{P}_{\mathbf{R}}^{\boldsymbol{\Psi}}\mathcal{P}_{\mathbf{B}}^{\mathbf{A}} = \mathcal{P}_{\mathbf{R}}^{\boldsymbol{\Psi}}\mathcal{P}_{\mathbf{B}}^{\mathbf{A}} = \mathcal{P}_{\mathbf{R}}^{\boldsymbol{\Psi}}\mathcal{P}_{\mathbf{B}}^{\mathbf{A}}\mathcal{P}_{\mathbf{R}}^{\boldsymbol{\Psi}} \tag{C.6}$$

where the first equality is a direct consequence of the idempotent property of $\mathcal{P}_{\mathbf{B}}^{\mathbf{A}}$*, but the second relation is less evident. A direct consequence of* (C.6) *is that* $\mathcal{P}_{\mathbf{R}}^{\mathbf{\Psi}}\mathcal{P}_{\mathbf{B}}^{\mathbf{A}}\mathcal{P}_{\mathbf{R}}^{\mathbf{\Psi}}\mathbf{AB}=\mathbf{0}$.

Corollary 3. *A complete space of vectors* $\boldsymbol{\lambda}\in\mathbb{R}^n$ *fulfilling the constraint* $\mathbf{R}^{\mathsf{T}}\boldsymbol{\lambda}=\mathbf{0}$*, can be expressed for example using a one-level decomposition equivalent to* (B.6) *in the form,*

$$\boldsymbol{\lambda} = \mathcal{P}_{\mathbf{R}}^{\mathbf{\Psi}}\left\{\mathcal{P}_{\mathbf{B}}^{\mathbf{A}}\boldsymbol{\alpha}+\mathbf{AB}\boldsymbol{\beta}\right\} \tag{C.7}$$

$$\boldsymbol{\lambda} = \mathcal{P}_{\mathbf{R}}^{\mathbf{\Psi}}\left\{\mathcal{P}_{\mathbf{B}}^{\mathbf{A}^{\mathsf{T}}}\boldsymbol{\alpha}+\mathbf{B}\boldsymbol{\beta}\right\} \tag{C.8}$$

or with a two-level decomposition similar to (B.8) *like,*

$$\boldsymbol{\lambda}=\mathcal{P}_{\mathbf{R}}^{\mathbf{\Psi}}\left\{\mathcal{P}_{\mathbf{C}}^{\mathbf{D}^{\mathsf{T}}}\left\{\mathcal{P}_{\mathbf{B}}^{\mathbf{A}^{\mathsf{T}}}\boldsymbol{\alpha}+\mathbf{B}\boldsymbol{\beta}\right\}+\mathbf{C}\boldsymbol{\gamma}\right\}. \tag{C.9}$$

Example 2. Given a constant vector $\mathbf{g}\in\mathbb{R}^m$, the space of all $\boldsymbol{\lambda}\in\mathbb{R}^n$ such that $\mathbf{B}^{\mathsf{T}}\boldsymbol{\lambda}=\mathbf{g}$ and fulfilling at the same time the condition $\mathbf{R}^{\mathsf{T}}\boldsymbol{\lambda}=\mathbf{0}$, can be represented as the one-level decomposition (C.7) as

$$\boldsymbol{\lambda}=\mathcal{P}_{\mathbf{R}}^{\mathbf{\Psi}}\left\{\mathcal{P}_{\mathbf{B}}^{\mathbf{A}}\boldsymbol{\alpha}+\mathbf{AB}\left[\mathbf{B}^{\mathsf{T}}\mathbf{AB}\right]^{-1}\mathbf{g}\right\} \tag{C.10}$$

with $\boldsymbol{\alpha}\in\mathbb{R}^n$.

References

[1] J. H. Argyris, S. Kelsey, Energy Theorems and Structural Analysis, Butterworths, London, 1955.

[2] K. Washizu, Variational Methods in Elasticity and Plasticity, Pergamon Press, New York, 1972.

[3] B. M. Fraeijs de Veubeke, Variational principles and the patch test, International Journal for Numerical Methods in Engineering 8 (1974) 783–801.

[4] S. N. Atluri, On 'hybrid' finite-element models in solid mechanics, in: R. Vichnevetsky (Ed.), Advances in Computer Methods for Partial Differential Equations, Rutgers University: AICA, 1975, pp. 346–356.

[5] J. T. Oden, J. N. Reddy, Variational Methods in Theoretical Mechanics, Springer-Verlag, 1982.

[6] C. A. Felippa, A survey of parametrized variational principles and applications to computational mechanics, Computer Methods in Applied Mechanics and Engineering 113 (1996) 109–139.

[7] R. Barrett, M. Berry, T. F. Chan, J. Demmel, J. Donato, J. Dongarra, V. Eijkhout, R. Pozo, C. Romine, H. van der Vorst, Templates for the Solution of Linear Systems: Building Blocks for Iterative Methods, SIAM Publications, Philadelphia, 1994.

[8] Y. Saad, Iterative Methods for Sparse Linear Systems, 2nd ed., SIAM Society for Industrial and Applied Mathematics, 2003.

[9] S. Balay, S. Abhyankar, M. F. Adams, J. Brown, P. Brune, K. Buschelman, L. Dalcin, A. Dener, V. Eijkhout, W. D. Gropp, D. Karpeyev, D. Kaushik, M. G. Knepley, D. A. May, L. C. McInnes, R. T. Mills, T. Munson, K. Rupp, P. Sanan, B. F. Smith, S. Zampini, H. Zhang, H. Zhang, PETSc Web page, https://www.mcs.anl.gov/petsc, 2019.

[10] K. C. Park, M. R. Justino, C. A. Felippa, An algebraically partitioned FETI method for parallel structural analysis: Algorithm description, International Journal for Numerical Methods in Engineering 40 (1997) 2717–2737.

[11] M. R. Justino, K. C. Park, C. A. Felippa, An algebraically partitioned FETI method for parallel structural analysis: Performance evaluation, International Journal for Numerical Methods in Engineering 40 (1997) 2739–2758.

[12] K. C. Park, C. A. Felippa, A variational framework for solution method developments in structural mechanics, Journal of Applied Mechanics 65 (1998) 242–249.

[13] U. A. Gumaste, K. C. Park, K. F. Alvin, A family of implicit partitioned time integration algorithms for parallel analysis of heterogeneous structural systems, Computational Mechanics 24 (2000) 463–475.

[14] K. C. Park, C. A. Felippa, U. A. Gumaste, A localized version of the metod of Lagrange multipliers and its applications, Computational Mechanics 24 (2000) 476–490.

[15] K. C. Park, C. A. Felippa, A variational principle for the formulation of partitioned structural systems, International Journal for Numerical Methods in Engineering 47 (2000) 395–418.

[16] M. R. Ross, C. A. Felippa, K. C. Park, M. A. Sprague, Treatment of acoustic fluid-structure interaction by localized Lagrange multipliers: Formulation, Computer Methods in Applied Mechanics and Engineering 197 (2008) 3057–3079.

[17] M. R. Ross, M. A. Sprague, C. A. Felippa, K. C. Park, Treatment of acoustic fluid-structure interaction by localized Lagrange multipliers and comparison to alternative interface-coupling methods, Computer Methods in Applied Mechanics and Engineering 198 (2009) 986–1005.

[18] A. A. Shabana, Dynamics of Multibody Systems, Cambridge University Press, Cambridge UK, 1998.

[19] K. C. Park, C. A. Felippa, R. Ohayon, Localized formulation of multibody systems, in: J. Ambrosio, M. Kleiber (Eds.), Computational Aspects of Nonlinear Systems with Large Rigid Body Motion, NATO Science Series, IOS Press, 2001, pp. 253–274.

[20] J. A. González, R. Abascal, K. C. Park, Partitioned analysis of flexible multibody systems using filtered linear finite element deformational modes, International Journal for Numerical Methods in Engineering 99 (2014) 102–128.

[21] C. Farhat, F. X. Roux, A method of finite-element tearing and interconnecting and its parallel solution algorithm, International Journal for Numerical Methods in Engineering 32 (1991) 1205–1227.

[22] C. Farhat, J. Mandel, F. X. Roux, Optimal convergence properties of the FETI domain decomposition method, Computer Methods in Applied Mechanics and Engineering 115 (1994) 365–385.

[23] C. Farhat, L. Crivelli, A transient FETI methodology for large-scale parallel implicit computations in structural mechanics, International Journal for Numerical Methods in Engineering 37 (1994) 1945–1975.

[24] C. Farhat, P. S. Chen, A scalable Lagrange multiplier based domain decomposition method for implicit time-dependent problems, International Journal for Numerical Methods in Engineering 38 (1995) 3831–3853.

[25] C. Farhat, J. Mandel, The two-level FETI method for static and dynamic plate problems. Part I: An optimal iterative solver for biharmonic systems, Computer Methods in Applied Mechanics and Engineering 155 (1998) 129–151.

[26] C. Farhat, P. S. Chen, J. Mandel, F. X. Roux, The two-level FETI method. Part II: Extension to shell problems, parallel implementation and performance results, Computer Methods in Applied Mechanics and Engineering 155 (1998) 153–179.

[27] C. Farhat, P. S. Chen, F. Risler, F. X. Roux, A unified framework for accelerating the convergence of iterative substructuring methods with Lagrange multipliers, International Journal for Numerical Methods in Engineering 42 (1998) 257–288.

[28] D. J. Rixen, C. Farhat, R. Tezaur, J. Mandel, Theoretical comparison of the FETI and Algebraically Partitioned FETI methods, and performance comparisons with a direct sparse solver, International Journal for Numerical Methods in Engineering 46 (1999) 501–533.

[29] M. Bhardwaj, D. Day, C. Farhat, M. Lesoinne, K. Pierson, D. Rixen, Application of the FETI method to ASCI problems-scalability results on 1000 processors and dicussion of highly heterogeneous problems, International Journal for Numerical Methods in Engineering 47 (2000) 513–535.

[30] C. Farhat, K. Pierson, M. Lessoine, The second generation FETI methods and their application to the parallel solution of large-scale linear and geometrically non-linear structural analysis problems, Computer Methods in Applied Mechanics and Engineering 184 (2000) 333–374.

[31] C. Farhat, M. Lessoine, P. LeTallec, K. Pierson, D. Rixen, FETI-DP: A dualprimal unified FETI method. Part I: a faster alternative to the two-level FETI method, International Journal for Numerical Methods in Engineering 50 (2001) 1523–1544.

[32] R. Molina, F. X. Roux, New implementations for the Simultaneous-FETI method, International Journal for Numerical Methods in Engineering 118 (2019) 519–535.

[33] M. Brun, A. Gravouil, A. Combescure, A. Limam, Two FETI-based heterogeneous time step coupling methods for Newmark and α-schemes derived from the energy method, Computer Methods in Applied Mechanics and Engineering 283 (2015) 130–176.

[34] S. S. Cho, R. Kolman, J. A. González, K. Park, Explicit multistep time integration for discontinuous elastic stress wave propagation in heterogeneous solids, International Journal for Numerical Methods in Engineering 118 (2019) 276–302.

[35] D. Dureisseix, C. Farhat, A numerically scalable domain decomposition method for the solution of frictionless contact problems, International Journal for Numerical Methods in Engineering 50 (2001) 2643–2666.

[36] P. Avery, G. Rebel, M. Lesoinne, C. Farhat, A numerically scalable dual-primal substructuring method for the solution of contact problems - part i: the frictionless case, Computer Methods in Applied Mechanics and Engineering 193 (2004) 2403–2426.

[37] C. Farhat, A. Macedo, M. Lesoinne, F. Roux, Two-level domain decomposition methods with lagrange multipliers for the fast iterative solution of acoustic scattering problems, Computer Methods in Applied Mechanics and Engineering 184 (2000) 213–239.

[38] K. C. Park, C. A. Felippa, R. Ohayon, Partitioned formulation of internal fluid-structure interaction problems via localized Lagrange multipliers, Computer Methods in Applied Mechanics and Engineering 190 (2001) 2989–3007.

[39] J. Li, C. Farhat, P. Avery, R. Tezaur, A dual-primal FETI method for solving a class of fluid-structure interaction problems in the frequency domain, International Journal for Numerical Methods in Engineering 89 (2011) 418–437.

[40] K. C. Park, C. A. Felippa, R. Ohayon, The d'Alembert-Lagrange principal equations and applications to floating flexible structures, International Journal for Numerical Methods in Engineering 77 (2009) 1072–1099.

[41] J. S. Przemieniecki, Theory of Matrix Structural Analysis, McGraw-Hill, 1968.

[42] B. M. Fraeijs de Veubeke, Matrix structural analysis, in: Lecture Notes for the International Research Seminar on the Theory and Application of Finite Element Methods, Univ. Waterloo, Calgary, Alberta, Canada, 1973.

[43] J. H. Argyris, S. Mlejnek, Die Methode der Finiten Elemente, volume I, II, III, Vieweg, Braunscheig, 1986, 1987, 1988.

[44] G. Verchery, Régularisation du système de l'équilibre des structures élastiques discretès, in: Comptes Rendus à l'Académie des Sciences, Paris, 1990, pp. 585–589.

[45] C. Farhat, F. Hemez, J. Mandel, Improving the convergence rate of a transient substructuring iterative method using the rigid body modes of its static equivalent, in: Structures, Structural Dynamics, and Materials Conference, 36 th and AIAA/ASME Adaptive Structures Forum, New Orleans, LA, 1995, pp. 996–1010.

[46] J. A. González, K. C. Park, A simple explicit-implicit finite element tearing and interconnecting transient analysis algorithm, International Journal for Numerical Methods in Engineering 89 (2011) 1203–1226.

[47] C. Farhat, J. Li, P. Avery, A FETI-DP method for the parallel iterative solution of indefinite and complex-valued solid and shell vibration problems, International Journal for Numerical Methods in Engineering 63 (2005) 398–427.

[48] J. Toivanen, P. Avery, C. Farhat, A multilevel FETI-DP method and its performance for problems with billions of degrees of freedom, International Journal for Numerical Methods in Engineering 116 (2018) 661–682.

[49] J. A. González, K. C. Park, C. A. Felippa, A formulation based on localized Lagrange multipliers for BEM-FEM coupling in contact problems, Computer Methods in Applied Mechanics and Engineering 197 (2008) 623–640.

[50] C. Farhat, M. Géradin, On the general solution by a direct method of a large-scale singular system of linear equations: application to the analysis of floating structures, International Journal for Numerical Methods in Engineering 41 (1998) 675–696.

[51] C. A. Felippa, K. C. Park, The construction of free-free flexibility matrices for multilevel structural analysis, Computer Methods in Applied Mechanics and Engineering 191 (2002) 2139–2168.

[52] H. V. Henderson, S. R. Searle, On deriving the inverse of a sum of matrices, SIAM Review 23 (1981) 53–60.

[53] C. A. Felippa, K. C. Park, M. R. Justino, The construction of free–free flexibility matrices as generalized stiffness inverses, Computers and Structures 68 (1998) 411–418.

[54] M. Benzi, G. H. Golub, J. Liesen, Numerical solution of saddle point problems, Acta Numerica 14 (2005) 1–137.

[55] J. Mandel, R. Tezaur, C. Farhat, A scalable substructuring method by lagrange multipliers for plate bending problems, SIAM Journal on Numerical Analysis 36 (1999) 1370–1391.

[56] G. Karypis, V. Kumar, A fast and highly quality multilevel scheme for partitioning irregular graphs, SIAM Journal on Scientific Computing 20 (1999) 359–392.

[57] Y. Fragakis, M. Papadrakakis, The mosaic of high-performance domain decomposition methods for structural mechanics. Part II: Formulation enhancements, multiple right-hand sides and implicit dynamics, Computer Methods in Applied Mechanics and Engineering 193 (2004) 4611–4662.

[58] C. A. Felippa, A study of optimal membrane triangles with drilling freedoms, Computer Methods in Applied Mechanics and Engineering 192 (2003) 2125 – 2168.

[59] Y. Fragakis, M. Papadrakakis, The mosaic of high performance domain decomposition methods for structural mechanics: Formulation, interrelation and numerical efficiency of primal and dual methods, Computer Methods in Applied Mechanics and Engineering 192 (2003) 3799–3830.

[60] J. Robinson, Integrated theory of finite element methods, Wiley, 1973.